00-1491

DECEMBER 19, 1966

THIRD QUARTERLY PROGRESS REPORT

RESEARCH STUDY ON INSTRUMENT UNIT THERMAL CONDITIONING HEAT SINK CONCEPTS

SEPTEMBER 1 TO NOVEMBER 30, 1966

PREPARED FOR

GEORGE C. MAKSHALL SPACE FLIGHT CENTER
HUNTSVILLII, ALABAMA
CONTRACT NO. NAS8-11291

GARRETT
AIRESEARCH MANUFACTURING DIVISION
Los Angeles, California

66-1491

DECEMBER 19, 1966

THIRD QUARTERLY PROGRESS REPORT

RESEARCH STUDY ON INSTRUMENT UNIT THERMAL CONDITIONING HEAT SINK CONCEPTS

SEPTEMBER 1 ~~TO~~ NOVEMBER 30, 1966

PREPARED FOR

GEORGE C. MARSHALL SPACE FLIGHT CENTER
HUNTSVILLE, ALABAMA
CONTRACT NO. NAS8-11291

Prepared by: D. W. Graumann

Edited by: R. A. Stone

Approved by: I. G. Austin

for F. E. Carroll

AIRESEARCH MANUFACTURING DIVISION
Los Angeles, California

CONTENTS

ILLUSTRATIONS

ILLUSTRATIONS (Continued)

THIRD QUARTERLY PROGRESS REPORT
RESEARCH STUDY ON INSTRUMENT UNIT
THERMAL CONDITIONING HEAT SINK CONCEPTS
SEPTEMBER 1 TO NOVEMBER 30, 1966

INTRODUCTION

This report reviews the work accomplished by the AiResearch Manufacturing Company, a division of The Garrett Corporation, Los Angeles, California between September 1 and November 30, 1966, under National Aeronautics and Space Administration Contract NAS 8-11291. This contract is for a research study on instrumentation unit thermal conditioning heat sink concepts. This report is the third quarterly progress report under the referenced contract which was signed on March 11, 1966. The previous report under this contract was issued under AiResearch Report No. 66-1376.

PROGRESS SUMMARY

During the third quarterly reporting period, work was accomplished in the following areas: Under Task I, Water Boiler Heat Sink Module, wick boiler modules were tested to determine the relative performance of rectangular and triangular fins. A new test module was designed and fabricated, and testing was continued. Vertical and horizontal wicking rate tests were performed. Under Task II, Water Sublimator Heat Sink Module, bench tests were performed on porous plates and a pressure drop correlation was developed. Single module sublimator tests were conducted to determine the performance of various porous plates. Under Task III, Thermal Conditioning Panel, preliminary panel designs were conceived and initial analyses begun.

TASK I: WATER BOILER HEAT SINK MODULE

Wick Heat Transfer and Performance Testing

Upon assembly of the single module wick boiler test apparatus, initial runs were made to calibrate the system for heat leak. This was done by supplying power to the electrical heaters while the unit contained no water. Several runs were made for power levels between 1 and 10 watts, and the system was allowed to come to temperature equilibrium. Temperature readings were taken at approximately 20-minute intervals, and from 3 to 5 hours were allowed

for equilibrium to be established. Data were obtained for plate temperatures up to 200°F. Subsequent testing indicated the heat losses to be, in all cases, less than 2 percent of the total heat transferred.

Two series of boiling tests were performed on similar units: one with rectangular fins between the wick and heater plates and the other with triangular fins. Both units were 4.5 in. high by 6 in. wide, contained 15 percent dense nickel fiber wicks, and had the fins brazed to the wicks. The wick in the rectangular finned unit was 0.090 in. thick, and the one in the triangular finned unit was 0.080 in. thick. Tests were performed at saturation temperatures of 40, 50, and 60°F, and heat fluxes as high as 8500 Btu per hr ft^2 were reached. Figures 1 and 2 show the results of two of these runs in the form of h vs AT, where AT is the difference between the heater plate temperature and the saturation temperature of the water. It is noted that there is a difference between the heat transfer coefficients at the top and bottom of the wick. (The thermocouple locations are 1 in. from the bottom and the top of the 4-1/2 in. module so that the boiling heat transfer coefficients are determined 2-1/2 in. apart.) The difference is more pronounced for the 50°F saturation temperature run than for the 40°F test. A difference in h would be expected at high values of heat flux due to the reduced capacity of the wick to deliver enough water to the upper portion of the wick. More precisely, at high heat fluxes, more of the water is boiled off at the bottom of the wick, so the water supply to the top of the wick is limited. This argument is supported by the fact that for $T_{sat} = 40°F$, the h at small heat fluxes is nearly the same for top and bottom, while at higher heat fluxes, the top h becomes less than the bottom h. However, at $T_{sat} = 50°F$, the top h is substantially less than the bottom h for even the small heat fluxes. Why this is true is not as yet known.

It is desired to compare the relative performance of rectangular and triangular fins. Figure 1 indicates that at $T_{sat} = 40°F$, there is essentially no difference in the two configurations with regard to the bottom h, but a slight difference with regard to the top h. For $T_{sat} = 50°F$, there is a slight difference for both the top and bottom h; however, the bottom h indicates the rectangular fin configuration gives better performance, and the

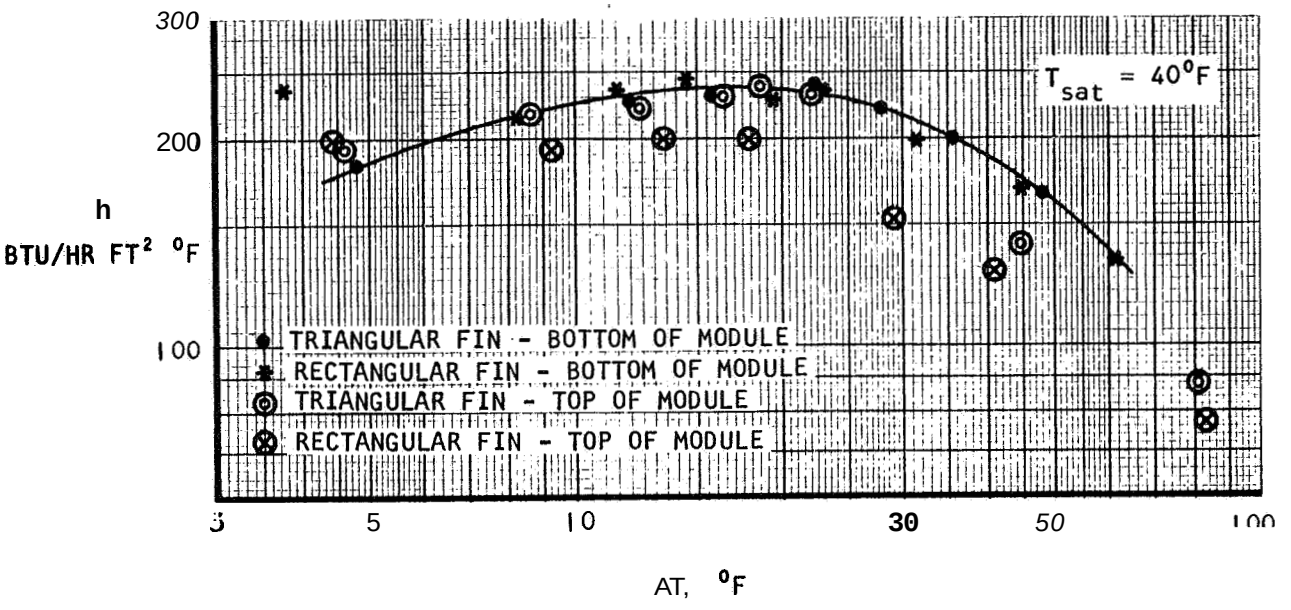

Figure 1. Performance of Single Module Wick Boiler

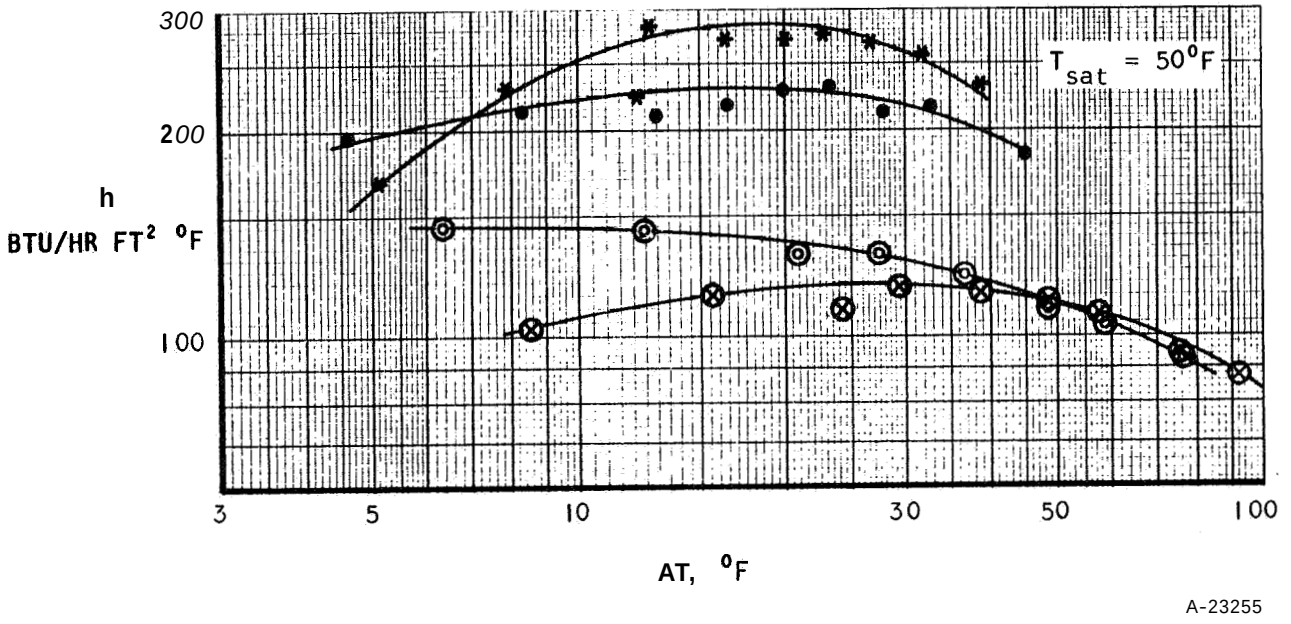

Figure 2. Performance of Single Module Wick Boiler

top h indicates the triangular fin is slightly better. It is probably safe to assume that any variations in performance between triangular and rectangular fins in this application will be slight.

Two problems were encountered which prompted a redesign of the wick boiler module. The first of these has been discussed, namely, the vertical variation in plate temperature (or h). These fairly large temperature differences cause substantial heat conduction in the vertical direction which may have a pronounced effect on the performance and the data obtained. The other problem is due to the relatively wide (6 in.) heater plates. For unbrazed modules, it is difficult to obtain good contact between the wick and fins at the middle of the wick due to a tendency of the wide plates to bow.

In order to eliminate the problems encountered, a new test module was designed and fabricated. Figure 3 shows components of the new heater plate assembly and Figures 4 and 5 show the assembled unit. The new design incorporates a series of heater plates, each thermally isolated from the next. Triangular fins are machined into the copper heater plates so the need for providing any additional heat transport surface is eliminated. Each copper plate has a copper constantan thermocouple imbedded in it and good thermocouple contact is assured by holding the thermocouple to the plate with a set screw as indicated in Figure 3. The three plates at the bottom of the module on each side contain two thermocouples located near the top and bottom of the plate; these will be used to verify the prediction of an essentially constant temperature in each plate. Eleven heaters on each side allow for the testing of wick samples 2 in. wide and up to 12 in. long. The separate heaters will eliminate any vertical conduction and will allow for varying the heat flux in the vertical direction as desired. Again, as with the previous design, various wick thicknesses may be tested since the horizontal heater spacing is adjustable.

The test setup is essentially the same as before with the module enclosed in a bell jar so low boiling temperatures may be obtained. Water is filtered and metered before entering the system and variable power input to the heaters is provided.

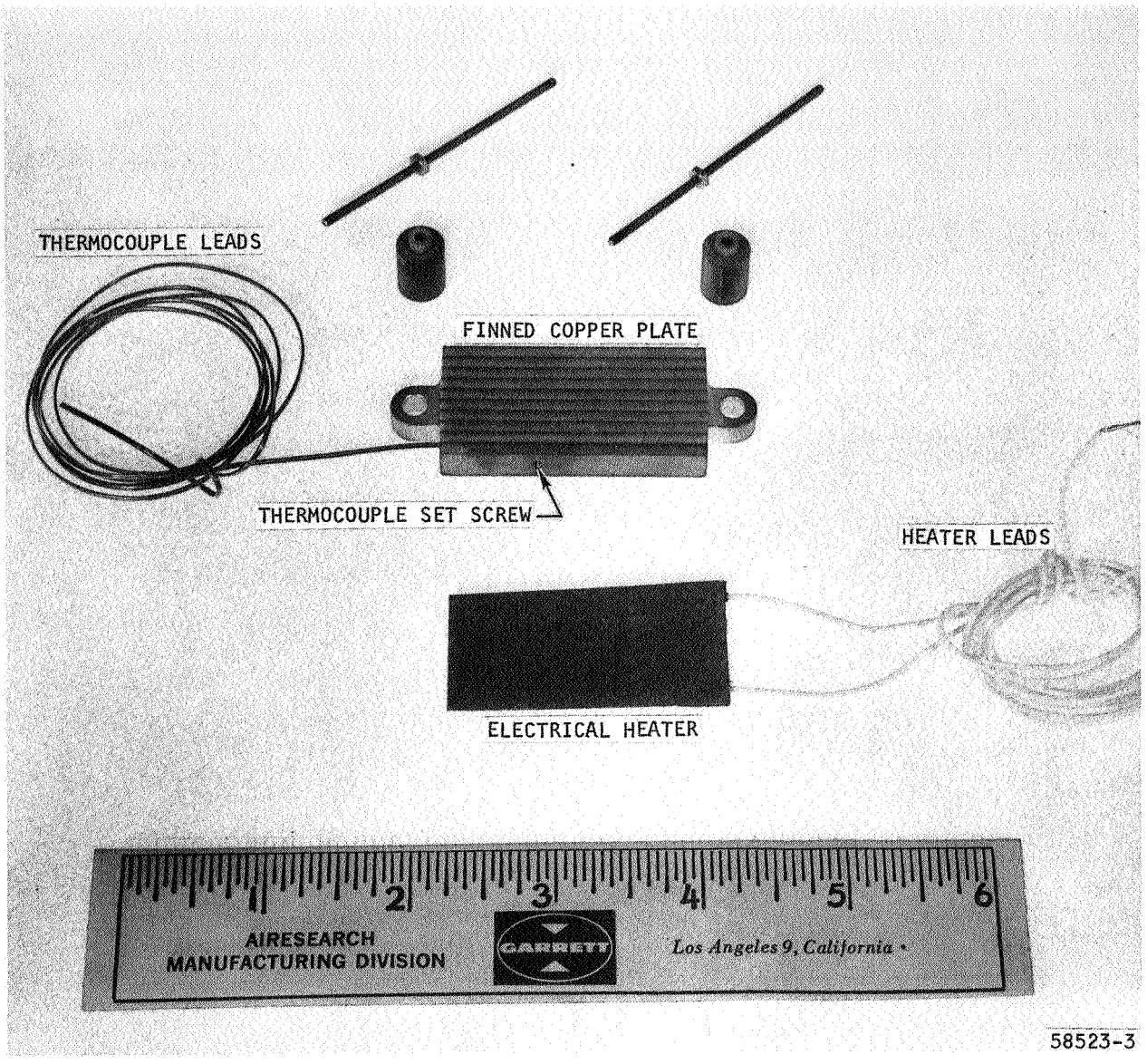

Figure 3. **Wick** Module Heater Plate Components

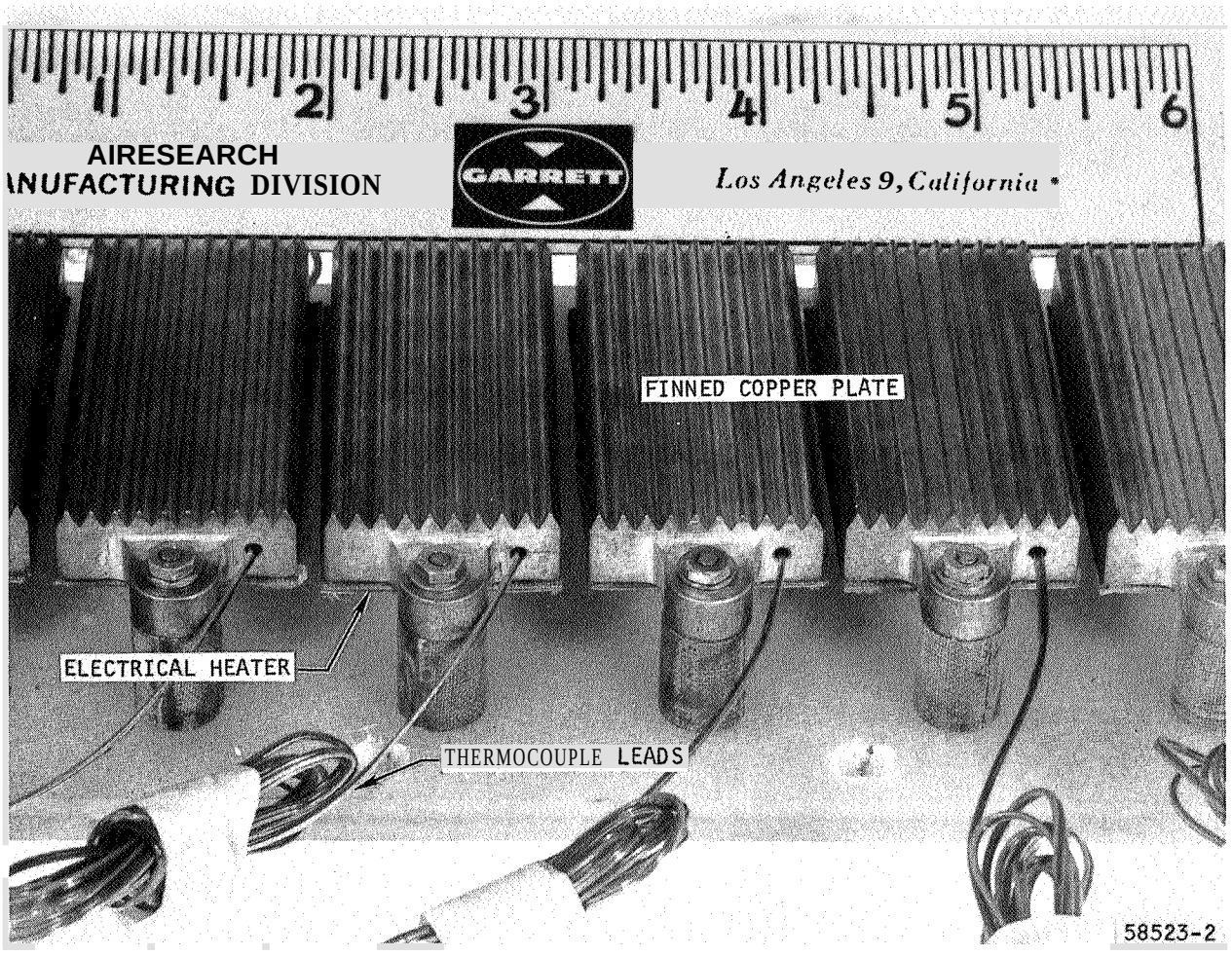

Figure 4. **Wick** Module Heater Plate **Assembly**

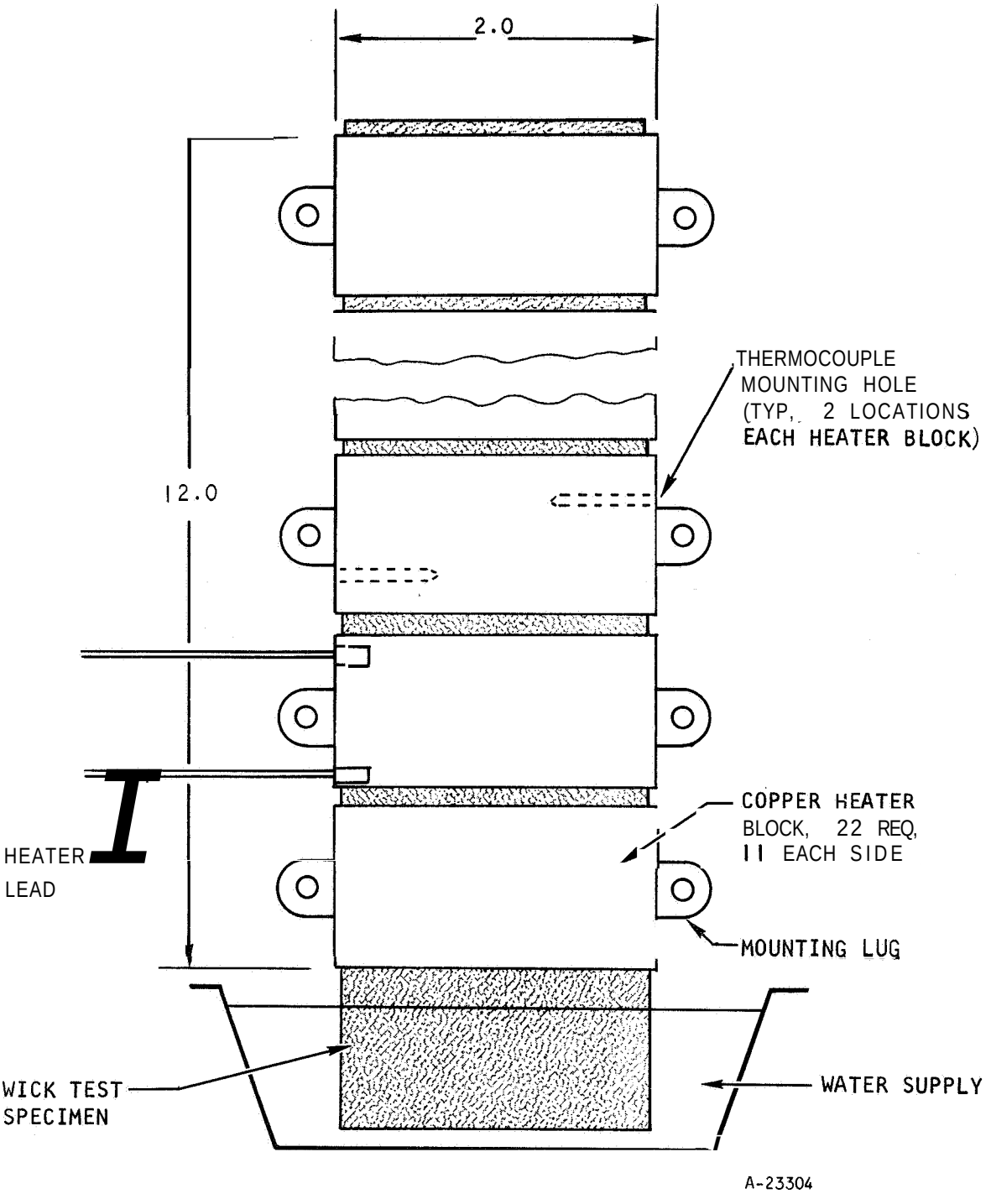

Figure 5. New Wick Performance Test Module

The test procedure involved setting a given heat flux and switching on the heaters, starting with those at the bottom and proceeding upward. Saturation temperature and heat flux were varied and the heater temperatures were recorded after each heater was turned on and the system had reached equilibrium.

Tests have been completed for a *0.090* in. thick, **15** percent dense nickel fiber metal wick for a saturation temperature of 40^0F and heat fluxes ranging from *900* Btu per hr ft^2 to *9000* Btu per hr ft^2. Figure 6 shows the effective h as a function of the difference between the heater temperature and the saturation temperature for various vertical positions on the wick. There does not appear to be a consistent difference between the coefficients obtained near the bottom and the top of the wick for this particular sample. A curve which most nearly approximates the data is shown as well as curves 20 percent above and below. As indicated, most of the data points lie within these 20 percent lines, representing good agreement for boiling data. The shape of the curve is similar to that obtained with data from the previous test rig. The effective boiling coefficient increases with increasing AT, peaks at about 15 to 20^0F AT and then decreases.

The data indicates that there is not a significant change in boiling performance at a certain position as additional heaters above it are switched on. Therefore, in future tests, all the heaters which do not exceed 200^0F will be switched on simultaneously, thereby reducing the test time significantly.

Wicking Height Tests

To aid in selection of optimum wicks for the boiler, vertical rise time and horizontal advance time tests were performed on the wicks listed on Page 12.

The results of these tests are given in Figures 7 and 8 where wicking height is shown as a function of time, It is difficult to obtain a consistent correlation between the results of these tests and the wick properties listed.

Error

An error occurred while processing this page. See the system log for more details.

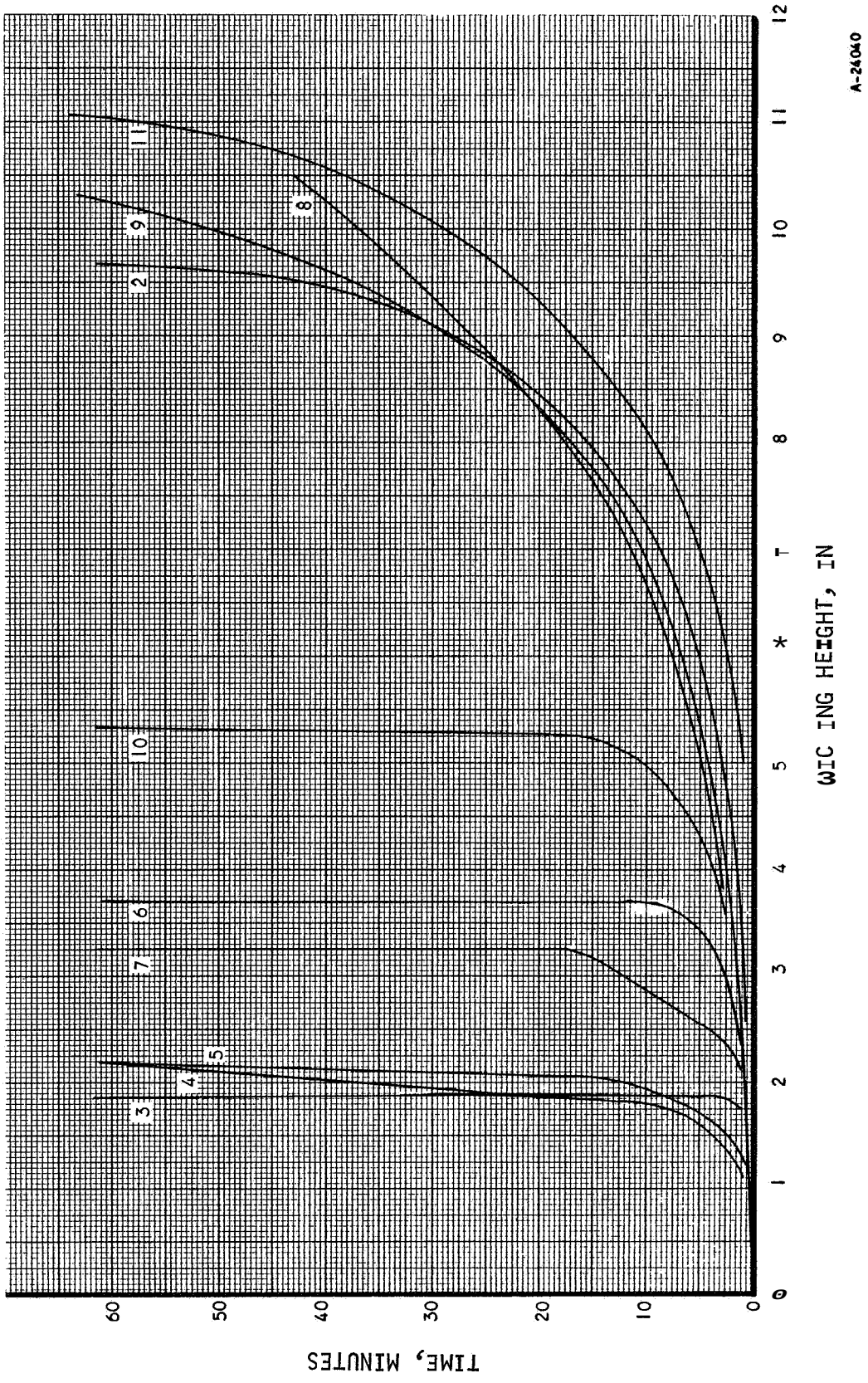

Figure 7. Vertical Wicking Rate of Test Specimens

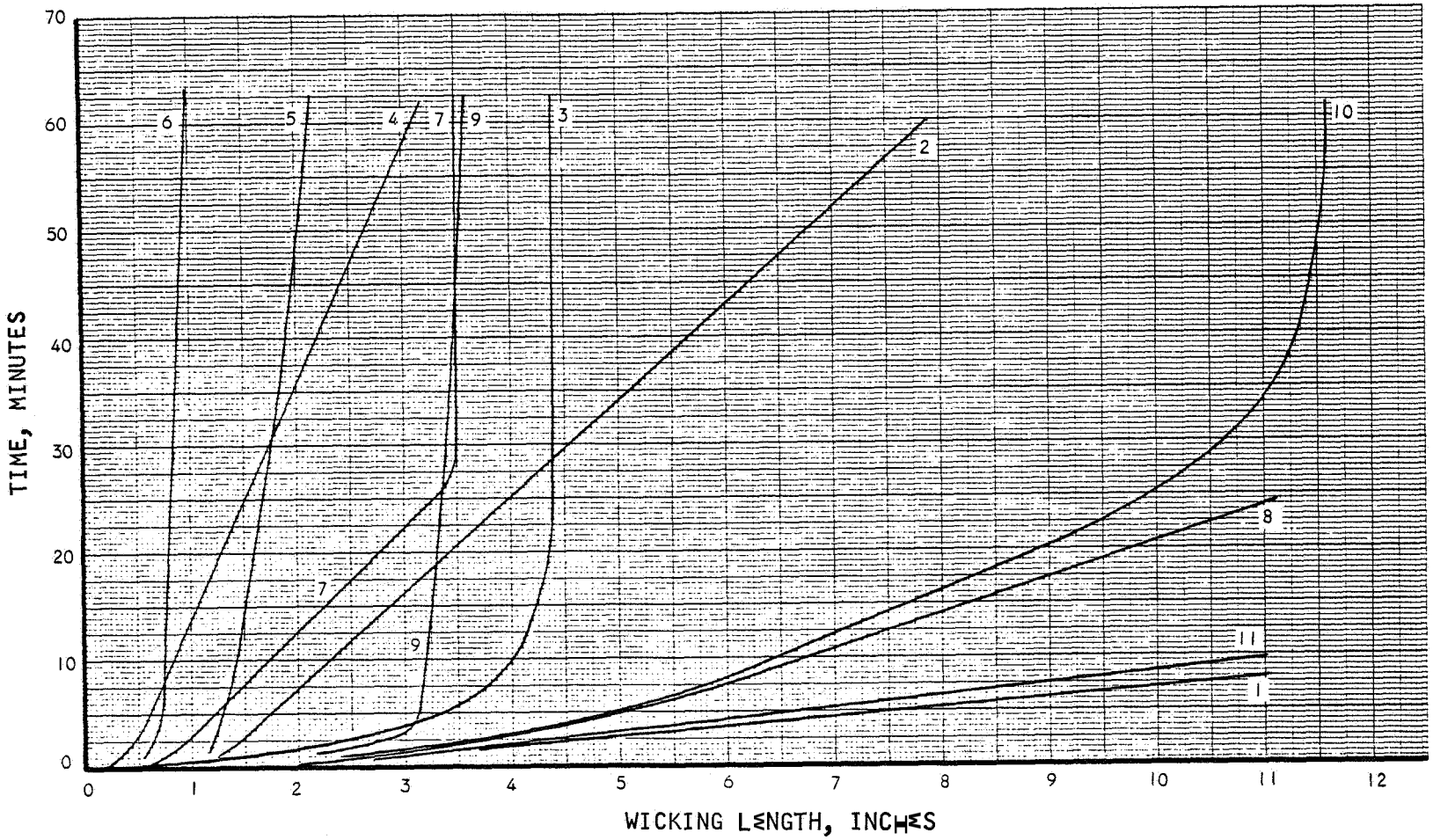

Figure 8. Horizontal Wicking Rate of Test Specimens

Wick Sample No.	Thickness, in.	Width, in.	Density, %
1	0.132	1.25	20
2	0.061	1.01	20
3	0.031	1.02	30
4	0.034	1.01	20
5	0.031	1.01	15
6	0.093	1.00	10
7	0.060	1.00	15
8	0.125	1.24	30
9	0.062	1.01	30
10	0.122	1.25	15
11	0.250	2.49	15

For the vertical rise time tests, it can be seen that the three thinnest wicks, 3, 4, and 5, gave the poorest performance from a final wick height standpoint, reaching a maximum height of about 2 in. For the other wicks, both the wicking rate and the ultimate wick height are functions of the density and thickness. This is especially true of the 15 percent dense wicks, Nos. 5, 7, 10, and 11, for which the wicking height increases significantly with increasing thickness. The strong dependence on thickness exhibited by some of the wicks may be the result of the forming process. The manner in which the wick is rolled and sintered during manufacturing may affect the pore size and structure near the surface. This would mean that the thicker wicks are less influenced by thickness than the thin ones.

The horizontal advance test results are shown in Figure 8. The theory indicates that the water in a horizontal wick should advance to the end of the wick, regardless of the length because there is no column of water which the capillary forces must support. Therefore, the vertical slopes shown for certain wicks are not expected and the data for these wicks are suspect. It would appear that the wicks were either contaminated or were structurally nonhomogeneous in such a manner as to limit flow. Some of the wicks do,

however, exhibit the expected tendency and continued to wick until either the top of the wick was reached or the test was terminated. Due to the fact that certain of these wicks did not perform as expected, they are being reCleaned and retested.

TASK 11: WATER SUBLIMATOR HEAT SINK MODULE

Porous Plate Bench Tests

A series of bench tests has been performed on *23* porous plates. A list of the plates tested is given in Table I, which includes plate identification, porosity, thickness, initial and *80* percent bubble points in alcohol, and the corresponding characteristic pore sizes. As indicated, all the plates tested in this series are nickel, ranging in thickness from 0.015 to 0.056 in. Porosities ranged from the smallest of *32* percent for one of the Union Carbide samples to 56.7 percent for a Clevite sample. All the specimens are of sintered particle construction, and Samples C1, C2, and C6 contain a 20 by 20 mesh, 0.007 in. diameter wire nickel reinforcement screen. The "L", "C", and "UC" designations refer to the Lockheed, Clevite, and Union Carbide Corporations, respectively, from whom this series of plates was obtained. Initial bubble points in alcohol were used to determine the maximum equivalent pore diameter of each plate. The Lockheed plates appear to have the smallest maximum pore diameters, about *2.5* microns, with approximately *80* percent of the pores larger than 1.5 microns. It will be shown below that these plates are the least permeable of all the plates tested. The Clevite plates have the largest pores of those tested in this series, from 6 to *8* microns. The Union Carbide plates have more of a spread in maximum equivalent pore diameter, from *2.82* to *6.90* microns, with the *80* percent pore diameters equal to from 57 to 76 percent of the maximum diameters.

Permeability data were also obtained for the three sets of porous plates, one series with nitrogen discharge to ambient, the other with nitrogen discharge to vacuum *(0.093* mm Hg abs to ***1.42*** mm Hg abs). The results of these tests are shown in Figures *9* and 10 with discharge to vacuum, and Figures 11 and 12 with discharge to ambient. It is seen that just as in pore size, the "L" and "C" series tend to be bunched while the "UC" series is spread over a range.

TABLE I

POROUS PLATE DESCRIPTION AND *BUBBLE* POINT DATA

Plate	Material	Thickness in.	Porosity percent	Initial Bubble Point in Alcohol psi	80% Bubble Point in Alcohol psi	Maximum Equivalent Pore Diameter microns	80% Equivalent Pore Diameter microns
L1A	Nickel	.030		5.75	8.20	2.25	1.58
L2A	Nickel	.030		5.30	8.65	2.44	1.50
L3A	Nickel	.030		5.35	8.40	2.42	1.54
L4A	Nickel	.030		5.25	8.30	2.47	1.56
L5A	Nickel	.030		4.80	8.64	2.70	1.50
C1	Nickel	.0526	56.7				
c2	Nickel	.0462	49.5	1.81	2.24	7.15	5.78
c3	Nickel	.0525	48.5	1.52	1.81	8.52	7.15
c4	Nickel	.0555	50.0	1.88	2.16	6.90	6.00
c5	Nickel	.0556	46.7	1.66	1.81	7.80	7.15
C6	Nickel	.0516	54.1	1.59	1.73	8.15	7.48
UC1A	Nickel	.020	48	2.92	4.26	4.43	3.04
UC1B	Nickel	.018	42				
UC1C	Nickel	.015	32	4.59	6.50	2.82	1.99
UC2A	Nickel	.024	47	1.91	2.67	6.79	4.85
UC2B	Nickel	.022	41	3.83	5.05	3.38	2.57
UC2C	Nickel	.028	32	4.62	8.15	2.80	1.59
UC3A	Nickel	.023	48	4.26	5.60	3.04	2.32
UC3B	Nickel	.020	44	2.64	3.68	4.91	3.52
UC3C	Nickel	.018	34	2.10	3.61	6.17	3.59
UC4A	Nickel	.024	48	1.88	2.56	6.90	5.07
UC4B	Nickel	.022	32	2.71	4.70	4.78	2.76
UC4C	Nickel	.020	29	3.72	6.14	3.48	2.11

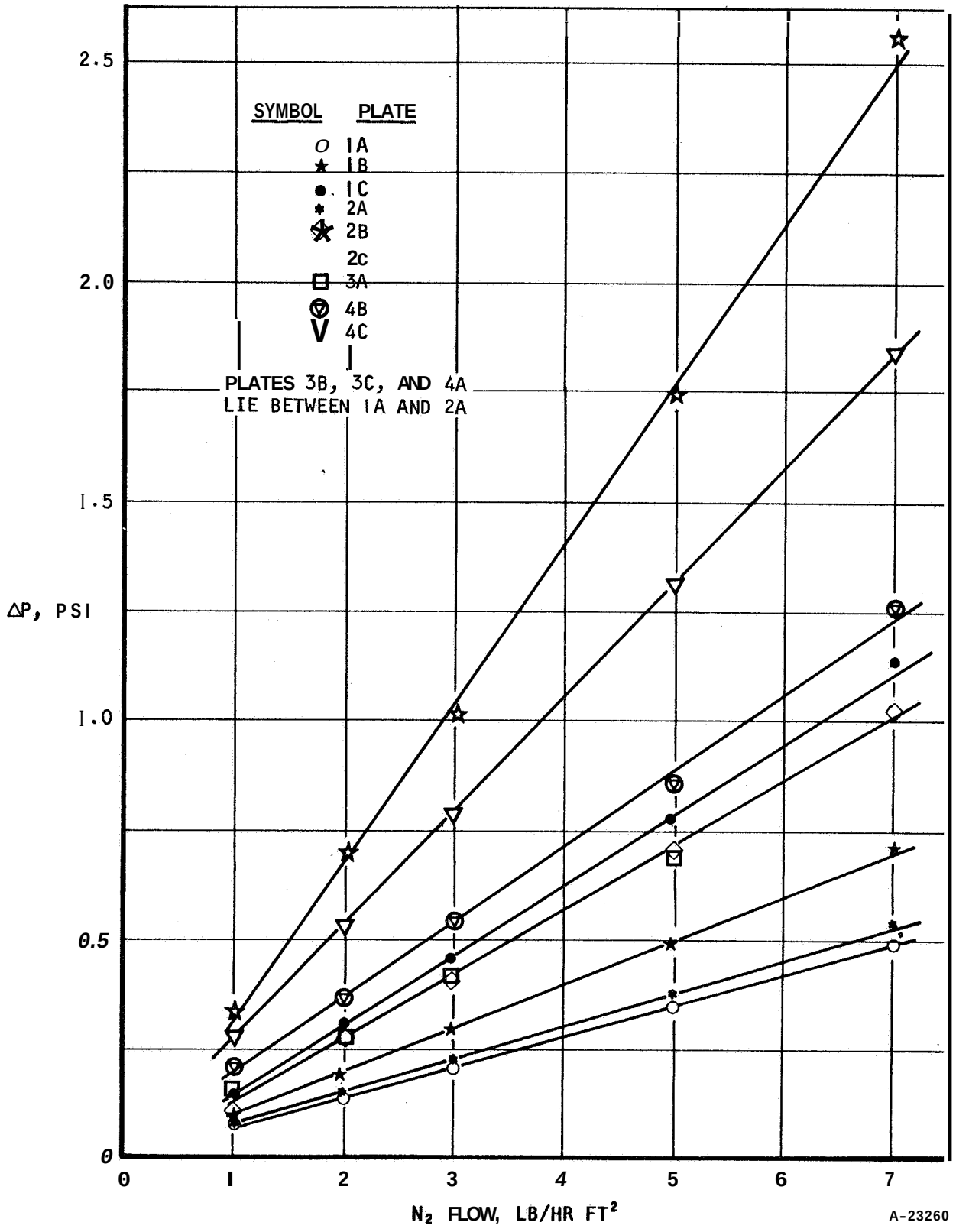

Figure 9. Nitrogen Permeability with Discharge to Vacuum

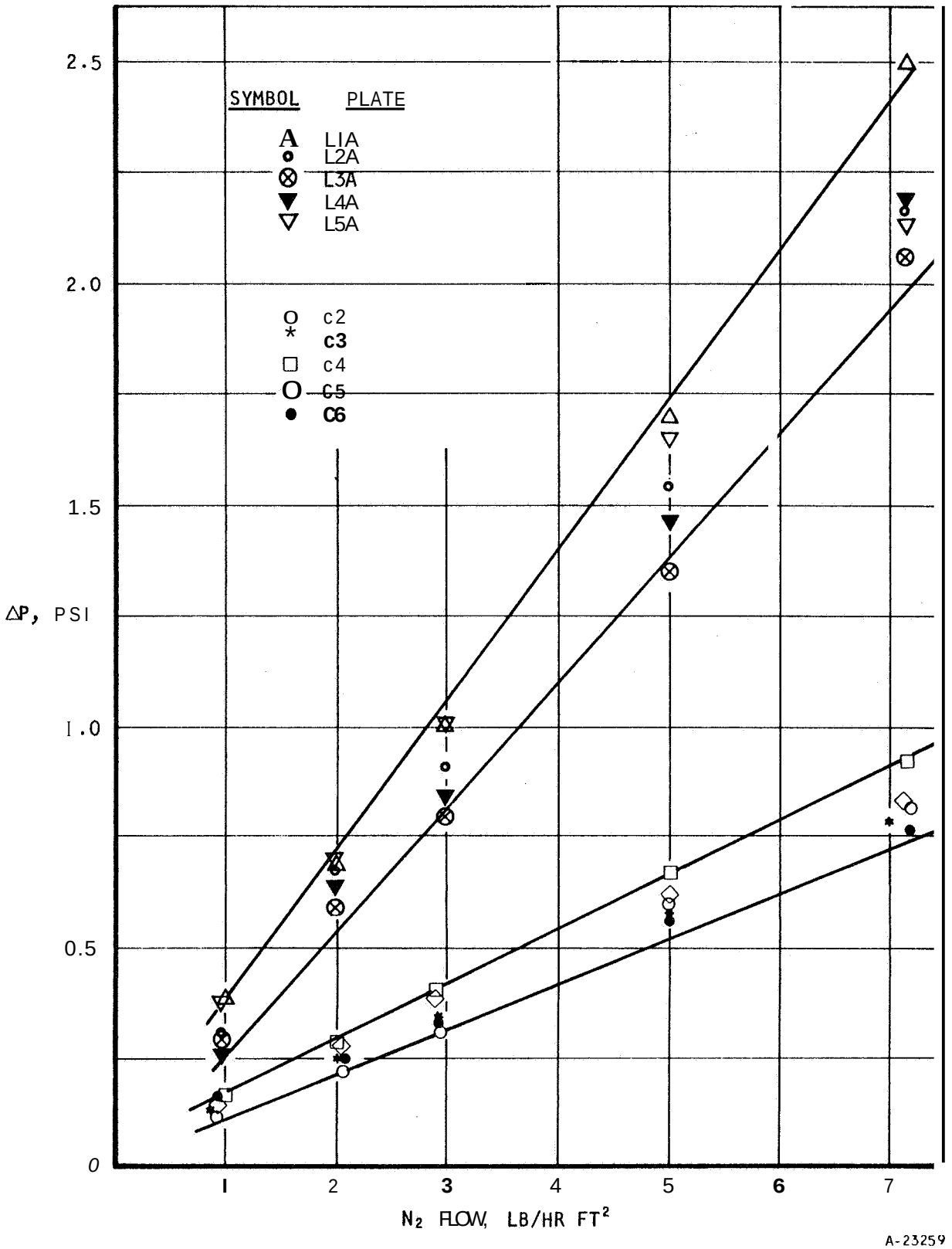

Figure 10. Nitrogen Permeability with Discharge to Vacuum

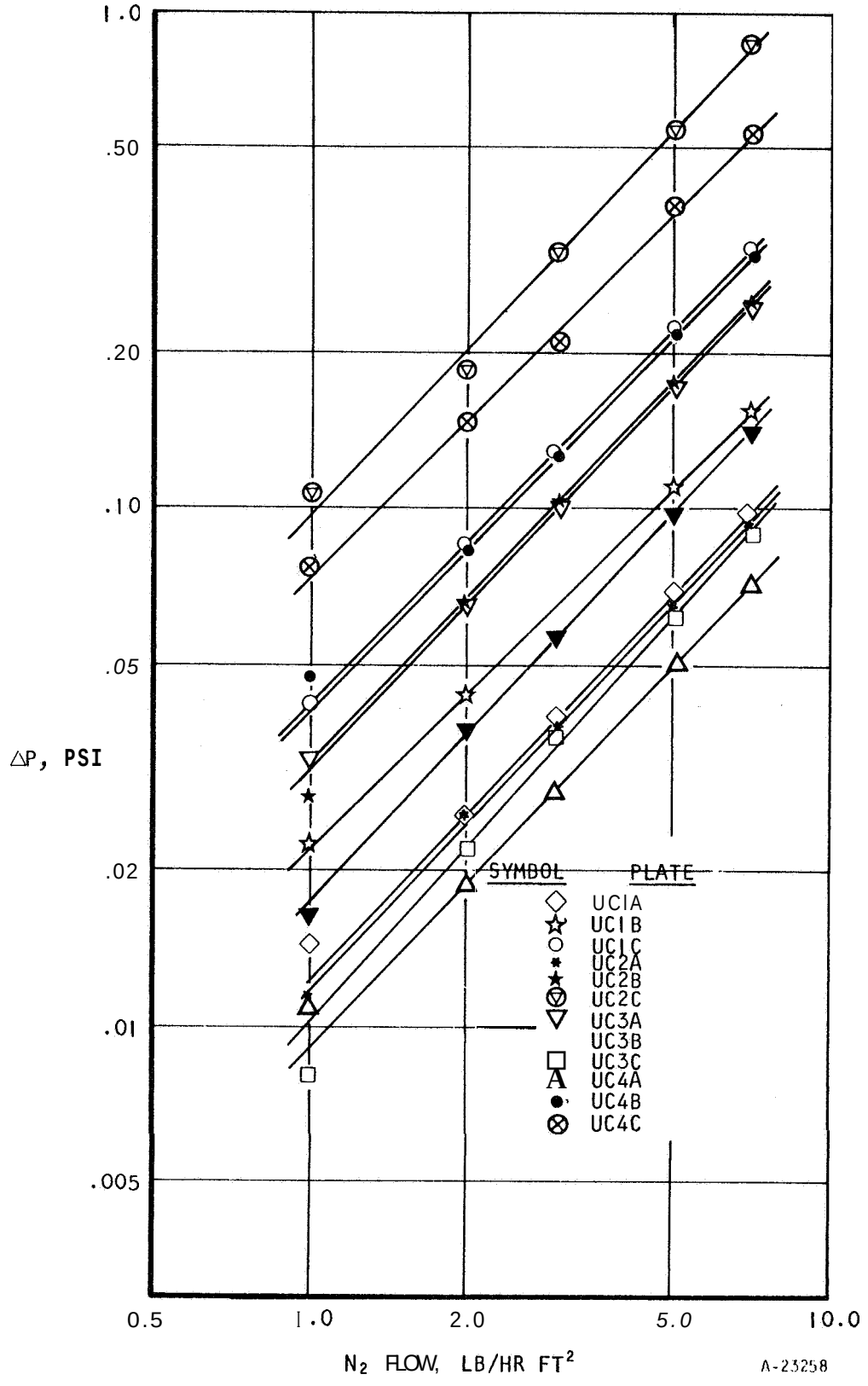

Figure 11. Nitrogen Permeability with Discharge to Ambient

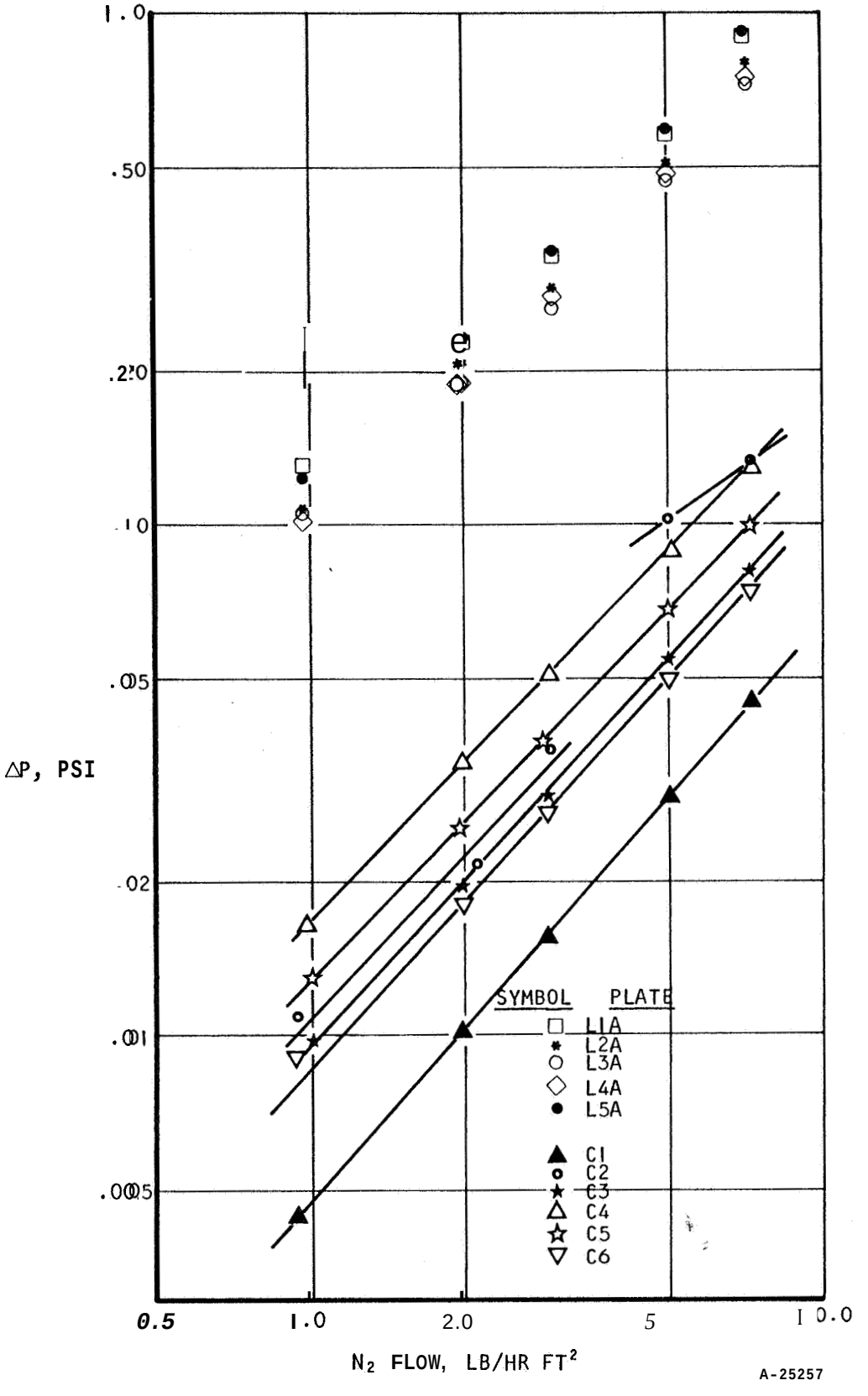

Figure 12. Nitrogen Permeability with Discharge to Ambient

It is obvious that for a sublimator plate application, a high degree of permeability is desirable. However, it is not known at this time what is the specific permeability requirement and, therefore, it is not possible to specify which (if any) of the plates tested are acceptable for this application. The sublimator performance test explained below should aid in fixing such a requirement.

It is of interest to note the correlation between permeability and pore size determined from bubble point tests. Below are listed the Union Carbide plates in order of increasing permeability for discharge to ambient with the corresponding maximum and 80 percent pore diameters. It is noted that although the correspondence is not exact, in general, the more permeable plates have the larger pore diameters. This would be expected for plates with essentially the same number of pores per unit area; as the holes get smaller, more pressure drop is required to force the gas through the plate.

Increasing Permeability	Maximum Equivalent Pore Diameter	80% Equivalent Pore Diameter
2C	2.80 μ	1.60 μ
4C	3.48	2.11
1C	2.82	2.00
4B	4.78	2.76
2B	3.38	2.57
3A	3.04	2.32
3B	4.91	3.52
1A	4.43	3.04
2A	6.79	4.85
3C	6.17	3.59
4A	6.90	5.07

Early in the test program, it became apparent that it would be necessary to obtain the permeability data at pressures comparable to those existing in an operating sublimator, pressures at or below the triple point of water (4.6 mm Hg abs). If data obtained at ambient conditions are extrapolated to very low pressures by use of the usual density correction, the pressure drops predicted are several orders of magnitude larger than experimentally

obtained values. It is apparent that gas rarefaction must be considered because of the very low ambient pressures to which the porous plates are exposed.

At ordinary pressures, gas intermolecular distances are much smaller than the body dimensions with which one is usually concerned in flow calculations and, therefore, the notion of a continuous gas is well fulfilled. At low pressures, with corresponding low densities, the molecular mean free path becomes comparable with body dimensions, and the effect of the molecular structure becomes a factor in flow and heat transfer mechanisms.

The relative importance of effects due to the rarefaction of a fluid may be indicated by a comparison of the magnitude of the mean free molecular path λ in the fluid with some significant body dimension. Hence, if ℓ is some characteristic body dimension in the flow field, the effect of rarefaction phenomena on flow and heat transfer will become important as soon as the ratio of λ/ℓ can no longer be neglected. This ratio is dimensionless and is referred to as the Knudsen number, Kn.

Three regimes of flow of gases may be distinguished: (1) continuum flow, in which the gas behaves as a continuous medium; (2) slip flow, in which the mean free path becomes significant and the gas velocity at the wall is no longer zero; and (3) free molecule flow, in which the mean free path is so great that intermolecular collisions are comparatively rare and are, therefore, less important than collisions with the wall. Various authors attach different values to the Knudsen numbers which divide the flow regimes. Tsien[1] proposed free molecule flow for Kn > 10, and Stalder[2] sets a limit of Kn > 2 with slip flow existing at Knudsen numbers somewhat smaller. The Knudsen number for flow in porous media can be expressed as

$$Kn = \frac{\lambda}{D_e} = \frac{\mu}{D_e P} \sqrt{\frac{\pi R T}{2 g_o}} \qquad (1)$$

[1] Tsien, H. S., Journal of the Aeronautical Sciences, *13, 653-664, 1946*

[2] Stalder, J. R., Goodwin, G., and Creager, M. O., "Heat Transfer to Bodies in a High Speed Rarefied Gas Stream," NACA TN *2438, 1951*

where μ = viscosity

R = gas constant

T = absolute temperature

P = pressure

g_o = conversion factor in Newton's law of motion = 32.2 $\frac{lb_m ft}{}$

D_e = equivalent pore diameter

At the water triple point pressure and temperature, the mean free path for water vapor is about 7 microns and about 10 microns for nitrogen gas. Therefore, for the equivalent pore diameters currently under consideration (1 to 8 microns), the Knudsen numbers range from about one to eight, and therefore the flow is in the free molecular and slip flow regimes.

It is desirable to obtain a correlation between pressure drop with ambient discharge and pressure drop with vacuum discharge. As stated above, it is not possible to correlate using density ratios due to the different flow regimes. Also, it is not possible to predict directly the pressure drops in either regime due to uncertainties in plate characteristics, such as free flow area and flow length. However, a fairly accurate correlation can be made by writing the pressure drop equations for the appropriate flow regimes and assuming flow through constant cross-section tubes.

The equation for pressure drop in a tube in free molecular flow is[3]:

$$\Delta P_{fm} = \frac{3}{8}\sqrt{\frac{\pi}{2}}\,\frac{CL}{A^2}\,\sqrt{\frac{RT_{fm}}{g_o}}\,W_{fm} \qquad (2)$$

where C = tube perimeter

A = free flow area

L = flow length

W = flow rate

[3]Roberts, J. K., Heat and Thermodynamics, p. 75, *1940.*

Using the definition of the equivalent diameter, $d_e = \frac{4A}{C}$, one obtains:

$$\Delta P_{fm} = 1.88 \sqrt{\frac{R\,T_{fm}}{g_o}} \frac{L}{d_e\,A}\, W_{fm} \qquad (3)$$

The expression for pressure drop in a tube in the continuum regime is:

$$\Delta P_c = \frac{4\,f\,l}{de} \frac{W_c^2}{2\,g_o\,\rho_c\,A^2} \qquad (4)$$

where f = friction factor

Due to the low flow rates involved and the linearity of test data, one can reasonably assume laminar flow and use the expression for friction factor:

$$f = \frac{C'}{Re} = \frac{C'\,\mu\,A}{W\,d_e} \qquad (5)$$

The value of C' varies with the shape of the tube cross section, and is 16 for a circular cross section and 13.3 for a triangular cross section. Since the porous plates are presumably formed of nearly spherical particles and the free flow area between three adjacent spheres is more nearly a triangle than a circle, it was decided to use a value of 13.3 in the analysis. Substituting Equation (5) into *(4)* and expressing ρ in terms of P, T, and R, one obtains:

$$\Delta P_c = \frac{26.6\,\mu_c\,R\,T_c}{P_c\,g_o} \frac{L}{d_e^2\,A}\, W_c \qquad (6)$$

Dividing Equation (3) by Equation *(6)* gives:

$$\frac{\Delta P_{fm}}{\Delta P_c} = 0.0707 \sqrt{\frac{g_o}{R}} \frac{T_{fm}}{T_c^2} \frac{P_c}{\mu_c}\, d_e\, \frac{W_{fm}}{W_c} \qquad (7)$$

As indicated, the free flow area terms vanish, and the only geometrical term remaining is d_e. Using the equivalent pore diameter obtained in bubble point tests, fairly good predictions for pressure drop in the free molecular flow regime can be made using continuum flow pressure drop data. The equivalent pore diameter obtained in bubble point tests is, strictly speaking, not identical to the equivalent diameter term appearing in Equation (7); however,

they are thought to be very nearly equal and, since it gives good agreement with experimental data, the bubble point equivalent diameter was used. The pore diameter which most closely characterizes the porous plate is neither the maximum D_e nor the 80 percent D_e, the maximum D_e being too large and the 80 percent D_e too small. Therefore, free molecular pressure drop predictions were based upon an average of the two D_e values. Figure 13 shows the vacuum discharge pressure drop predictions and experimental data for two porous plates, as well as the ambient discharge pressure drop experimental values from which pressure drop predictions were made. The two plates shown exhibit the best and the worst agreement between predictions and experimental data obtained in these tests. Table 2 shows the ratio of the experimental vacuum discharge pressure drops to the predicted pressure drops for all data points taken in this series. Fifty-one percent of the pressure drop data points taken with vacuum discharge were within 10 percent of the predicted values, and 85 percent were within 20 percent of the prediction.

Sublimator Performance Testing

In order to determine the performance of various porous plates in a sublimator, and to correlate the performance with bench tests, a sublimator module test apparatus was designed and assembled. The single porous plate module is similar in principle to the sublimation visualization test module described in previous reports in that it consists of a heat source, a finned water passage and a porous plate. The heat source is an electrical heater so that precise control of the input heat flux may be maintained. The unit is instrumented with 6 thermocouples in the heater plate and one at the water inlet, and continuous temperature readout is provided. The porous plate module installed in the test rig is shown in Figure *14.* For some of the thinner porous plate specimens, it was necessary to attach additional cross bar supports to prevent the plates from bowing as shown in the photograph. Not shown, but important to prevent heat losses, are the layers of aluminized mylar placed on the bottom of the module next to the heater plate. The three tubes on the left side of the module are additional water plenum inlet tubes which may be used in future testing, and the near tube is a water plenum pressure tap. A photograph of the test setup is shown

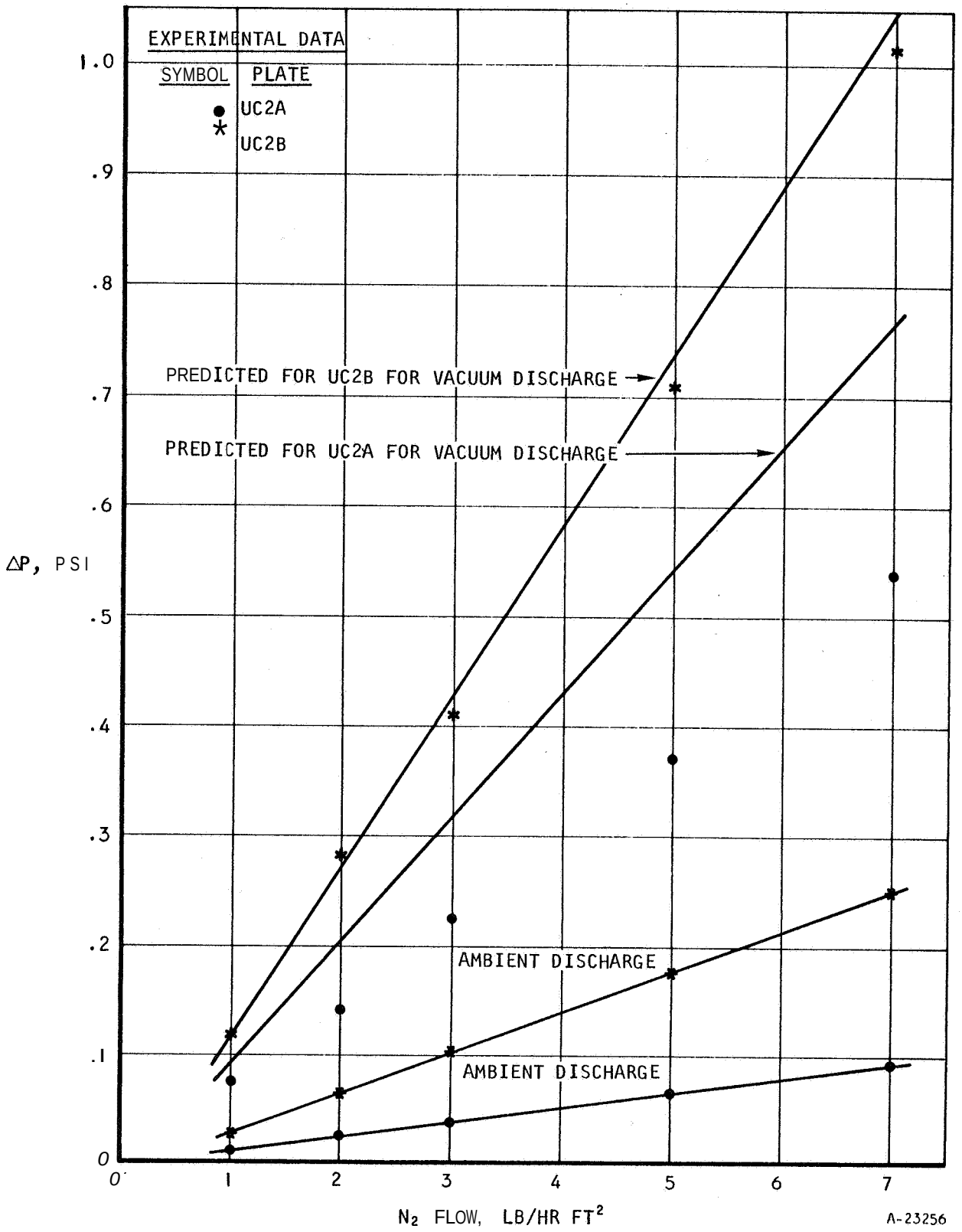

Figure 13. Predicted and Experimental Vacuum Discharge Pressure Drops

TABLE 2

RATIO OF EXPERIMENTAL VACUUM DISCHARGE ΔP
TO PREDICTED VACUUM DISCHARGE ΔP

	Flow Rate, lb/hr ft² plate				
Plate	1	2	3	5	7
L1A	1.07	1.11	1.11	1.07	1.04
L2A	1.04	1.18	1.11	1.07	1.04
L3A	1.00	1.11	1.11	1.07	1.04
L4A	.90	1.14	1.07	1.03	1.00
L5A	1.03	1.03	1.00	.93	.83
C2	1.20	1.12	.95	.65	.67
C3	1.24	1.13	1.07	.97	.88
C4	1.11	.91	.90	.82	.78
C5	1.08	1.08	.93	.87	.80
C6	1.58	1.24	1.13	1.02	.95
UC1A	1.06	1.02	.96	.94	.98
UC1C	1.03	1.09	1.06	1.03	1.06
UC2A	.83	.68	.72	.70	.71
UC2B	1.00	1.02	.95	.96	.96
UC2C	1.03	1.13	1.10	1.03	1.06
UC3A	1.26	1.16	1.08	1.05	
UC3B	.80	.81	.84	.83	.83
UC3C	1.34	.96	.85	.84	.84
UC4A	.75	.82	.80	.79	.79
UC4B	.84	.83	.80	.75	.77
UC4C	.94	.92	.93	.90	.89

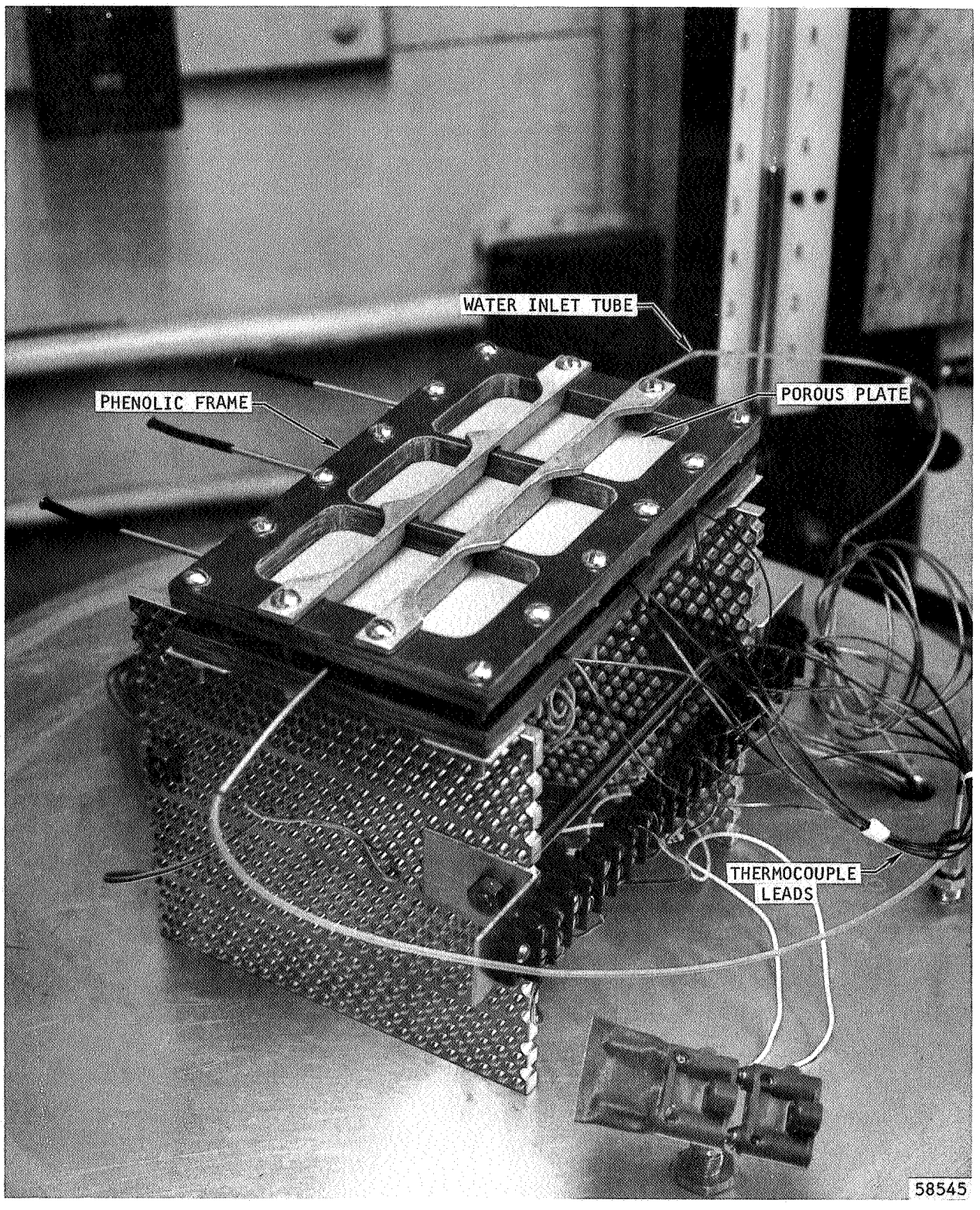

F-6291

Figure 14. Sublimator Test Module

in Figure 15. The electrically heated test modules are enclosed in a vacuum chamber in order to maintain the vapor pressure below the triple point. Heat flux is controlled by a variac, and voltage and current are indicated on appropriate meters. Water from the supply tank is filtered through a 1/2 μ absolute filter and metered before entering the sublimator module.

Initial tests were performed to determine the heat rejection capability of the various plates as a function of heater plate temperature and to determine the effects of feed water pressure and heat flux on breakthrough. The tests were performed at ambient pressures of from 80 to 850 microns of mercury absolute and heat fluxes were increased in incremental values until breakthrough occurred or until system power limitations were reached. The water plenum pressure was maintained at 3.7 psia. For some of the plates it was necessary to control the water flow at startup in order to prevent breakthrough. This is a problem which will undoubtedly require additional testing to determine pressure and flow rate limits for successful startup.

Two types of breakthrough occurred in the tests. One was the "uncontrolled" type which was characterized by water rushing through in such quantities as to flood and freeze the entire upper surface of the plate, thereby terminating the test, and the other was a "self-healing" type which was characterized by thin "ice fingers" or "ice sheets" appearing on the porous plate which in time sublimed away. The tests were run to investigate the "uncontrolled" breakthrough.

Figures 16, 17, and 18 show the results of these tests for some of the sample plates. As indicated, the UC-1 series all experienced breakthrough before the maximum system heat flux was reached. The figures indicate the last incremental heat flux reached before breakthrough. For this series some limited breakthrough did occur at lower heat fluxes, however, this was of the "self-healing" type. The UC-2 series did not experience uncontrolled breakthrough up to a heat flux of about 11,600 Btu per $hr\text{-}ft^2$, the power limit of the test setup. Limited "self-healing" breakthrough occurred on plates 2A and 2B at the higher heat fluxes, but none occurred on plate 2C for all heat fluxes. All the plates in the UC-3 series experienced uncontrolled breakthrough. Of the plates in the UC-4 series, only plate A

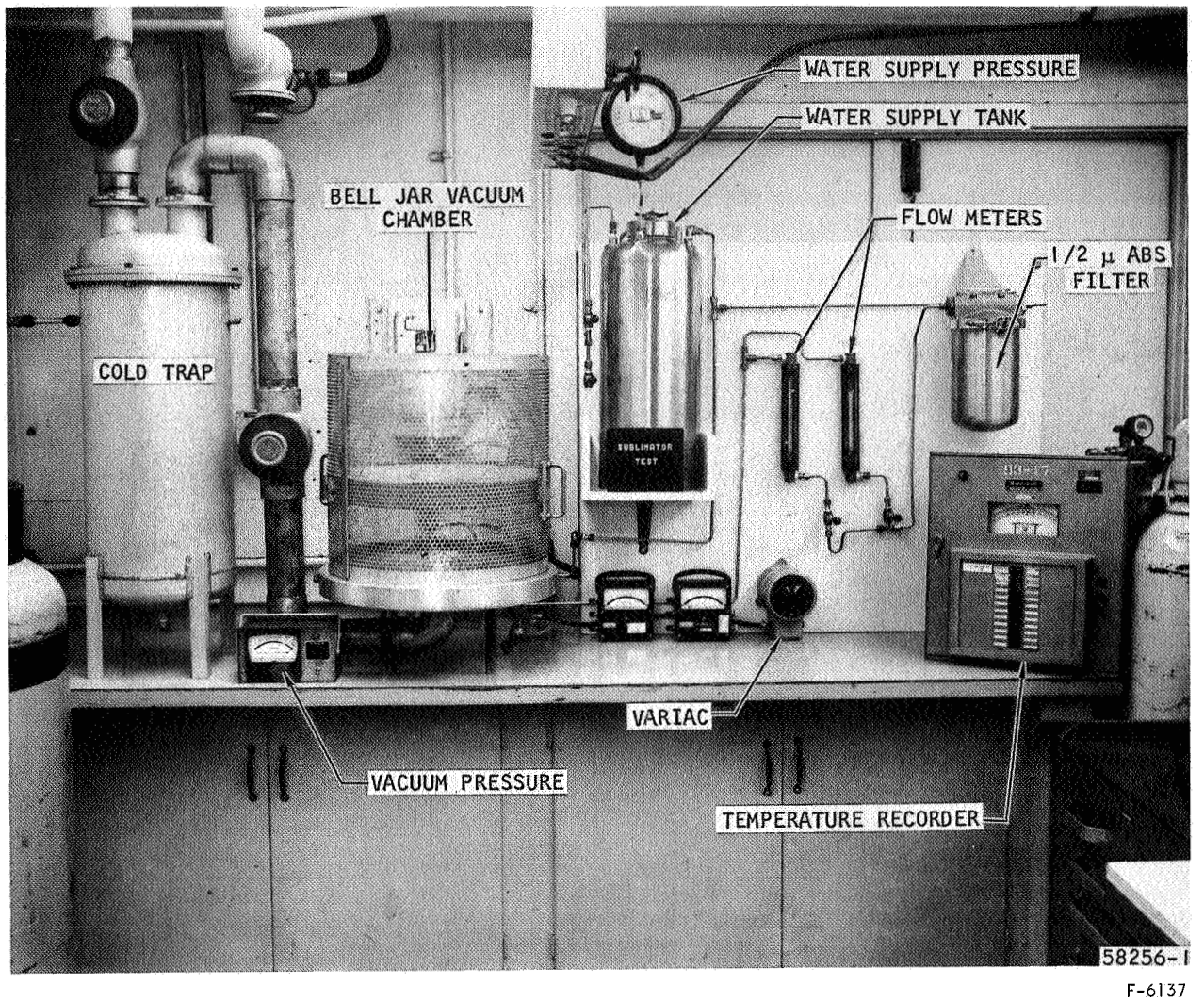

F-6137

Figure 15. Sublimator Performance Test Setup

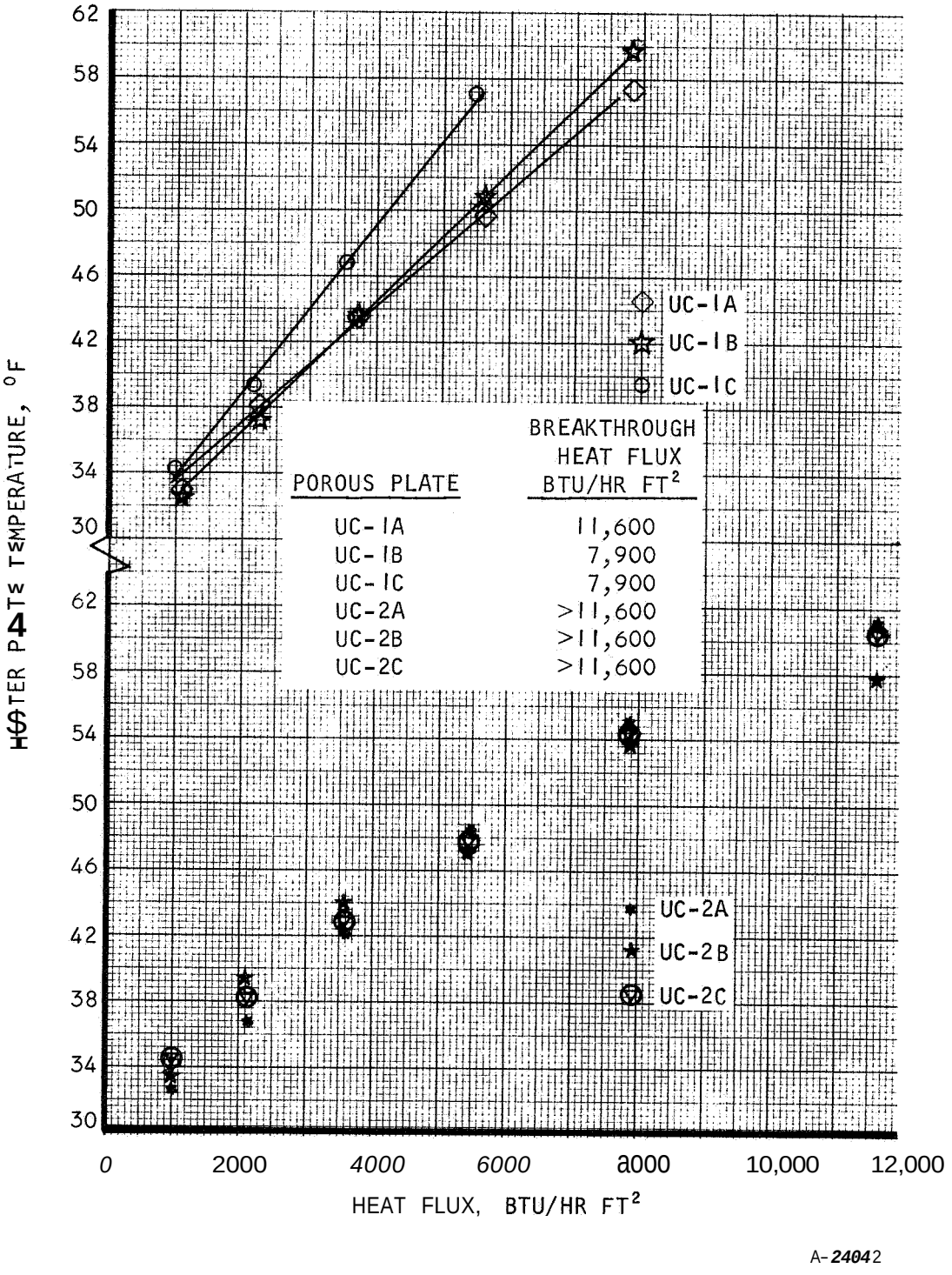

Figure 16. Single Hodule Sublimator Performance

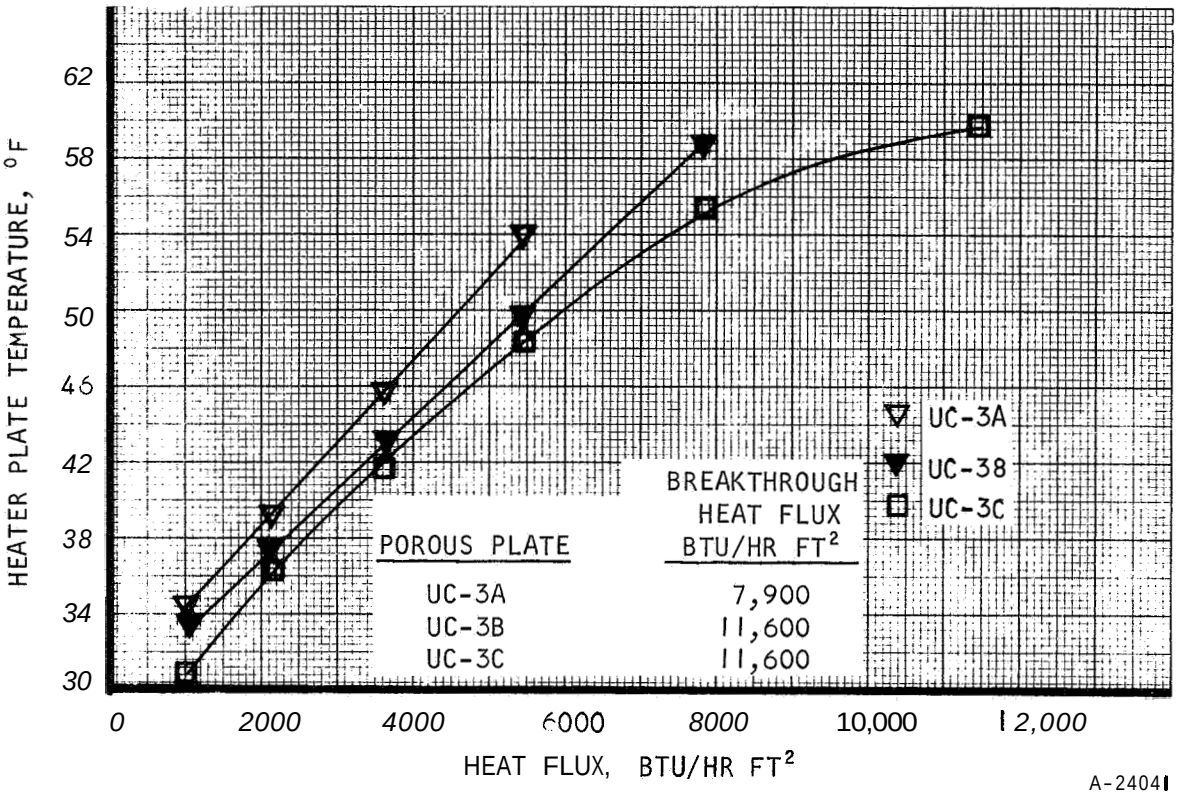

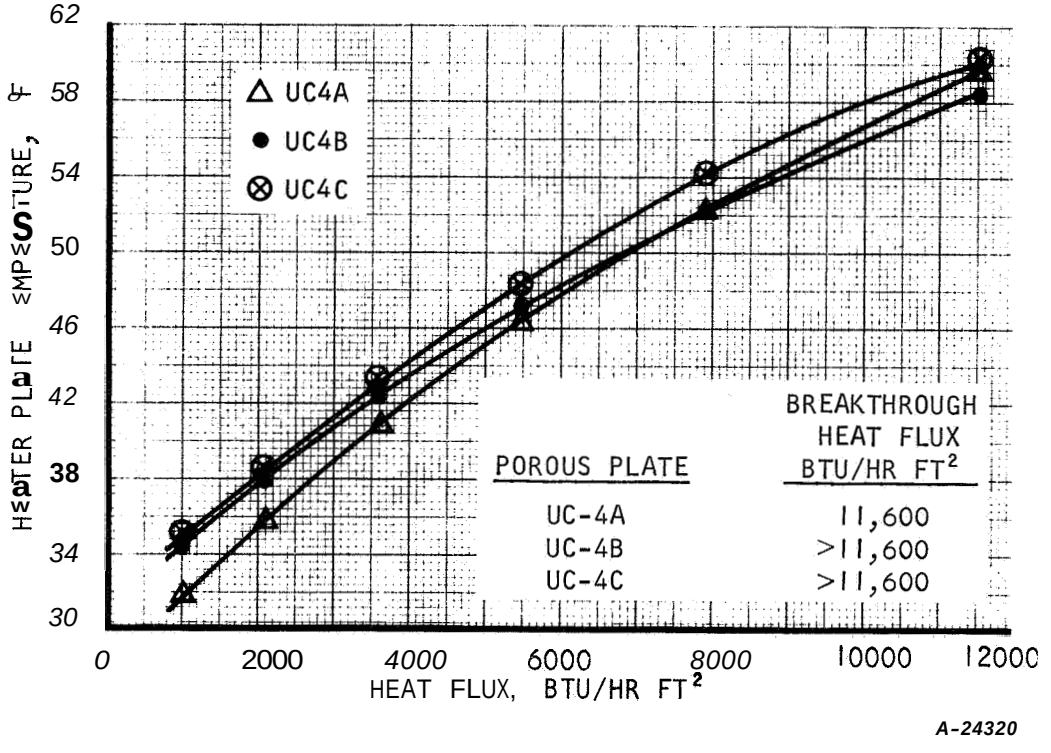

Figure 17. Single Module Sublimator Performance

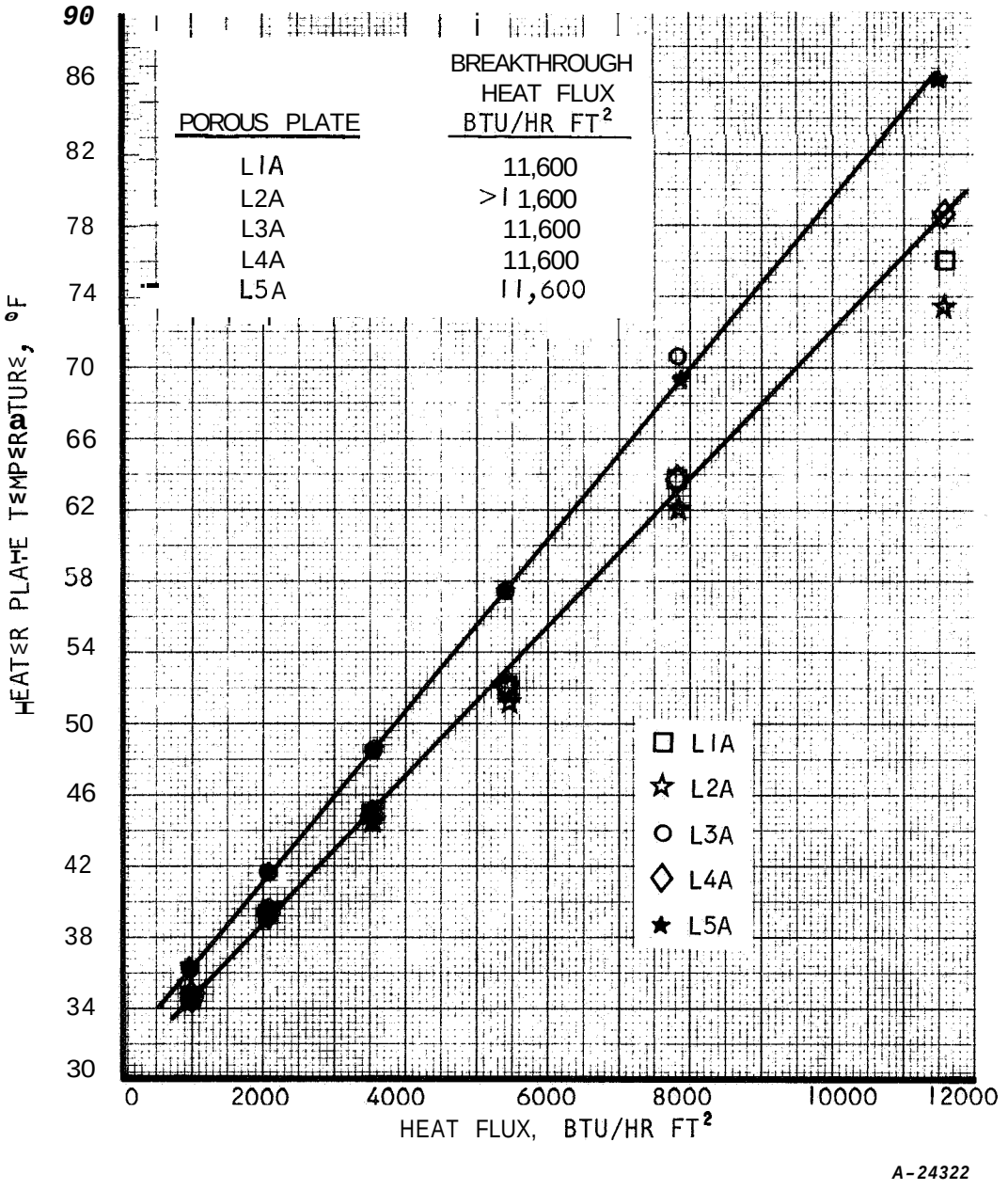

Figure 18. Single Module Sublimator Performance

experienced uncontrolled breakthrough and this was at the high heat flux. All the Lockheed plates except for plate 2A experienced uncontrolled breakthrough.

An attempt was made to correlate these breakthrough data on the basis of representative pore size and permeability, and although this has not as yet been successful on a gross basis, it was successful within each numbered series. The UC-2 series of plates which did not experience uncontrolled breakthrough ranged from the most to the least permeable and from the largest to the smallest pore size as indicated in Table I and Figure 9. The UC-I series covered a range in pore size and permeability not quite so extensive as the UC-2 series, and the plate with the smallest pores and lowest permeability broke through at the lowest heat flux. In the UC-3 series, again the least permeable plate with the smallest pores broke through at the lowest heat flux. Within series I and 3, two trends were observed: (I) the less permeable the plate, the higher the heater temperature at a given heat flux and (2) the less permeable the plate, the lower the heat flux at which breakthrough occurs. These trends did not extend from one series to the next however.

The only known similarity between plates in the same series is the starting powder from which the plate is sintered. This appears to be of some importance in the plate's performance; however, the complete significance of this fact is not understood as yet.

The exact heater plate temperature obtained at the various heat fluxes is not a significant factor, for this may be varied by placing a different fin in the water passage, however the temperatures relative to one another for the various plates do give some indication of their relative performance. The tests shown were conducted with a 0.100 in. high nickel fin with 20 fins per inch in the water passage. This fin and the water in the passage composed a significant portion of the heat transfer resistance, accounting for from 1/2 to 3/4 of the temperature drop. More significant in these tests was the determination of the breakthrough heat fluxes for the various porous plates.

THERMAL CONDITIONING PANEL

Conceptual design studies were initiated to develop possible thermal panel configurations. It was desired to obtain designs which meet the following system requirements:

a. The panel should have minimal control and supporting equipment requirements.

b. The panel should be capable of handling varying heat loads as well as long quiescent periods.

c. The panel should be capable of operating independent of the spacecraft cooling system.

Schematics of the various preliminary concepts are shown below with brief descriptions of the operation of the units.

Simple Sublimator System

A simple sublimator thermal panel concept is shown in Figure 19. This design consists of a water passage between the cold plate and several porous plates with water supplied from a bladder tank. When a heat load is applied to the cold plate, a solenoid valve is opened, allowing water to flow into the water passage where it freezes and sublimes. Restarting the system after a period of zero heat load would be possible if after closing the solenoid valve there were an adequate amount of residual heat in the experimental equipment.

If the heat load on the cold plate were highly nonuniform, a more uniform wall temperature may be obtained by one of two ways. One method would be to include in the system a small battery operated pump which would circulate the water in the manifold, thereby evening out any wall temperature variations. The other method would be to isolate the various porous plates over the face of the cold plate, providing each with its own solenoid valve but supplied from the same water tank. Appropriate design of the finned water passages could provide uniform plate temperatures for nonuniform heat fluxes.

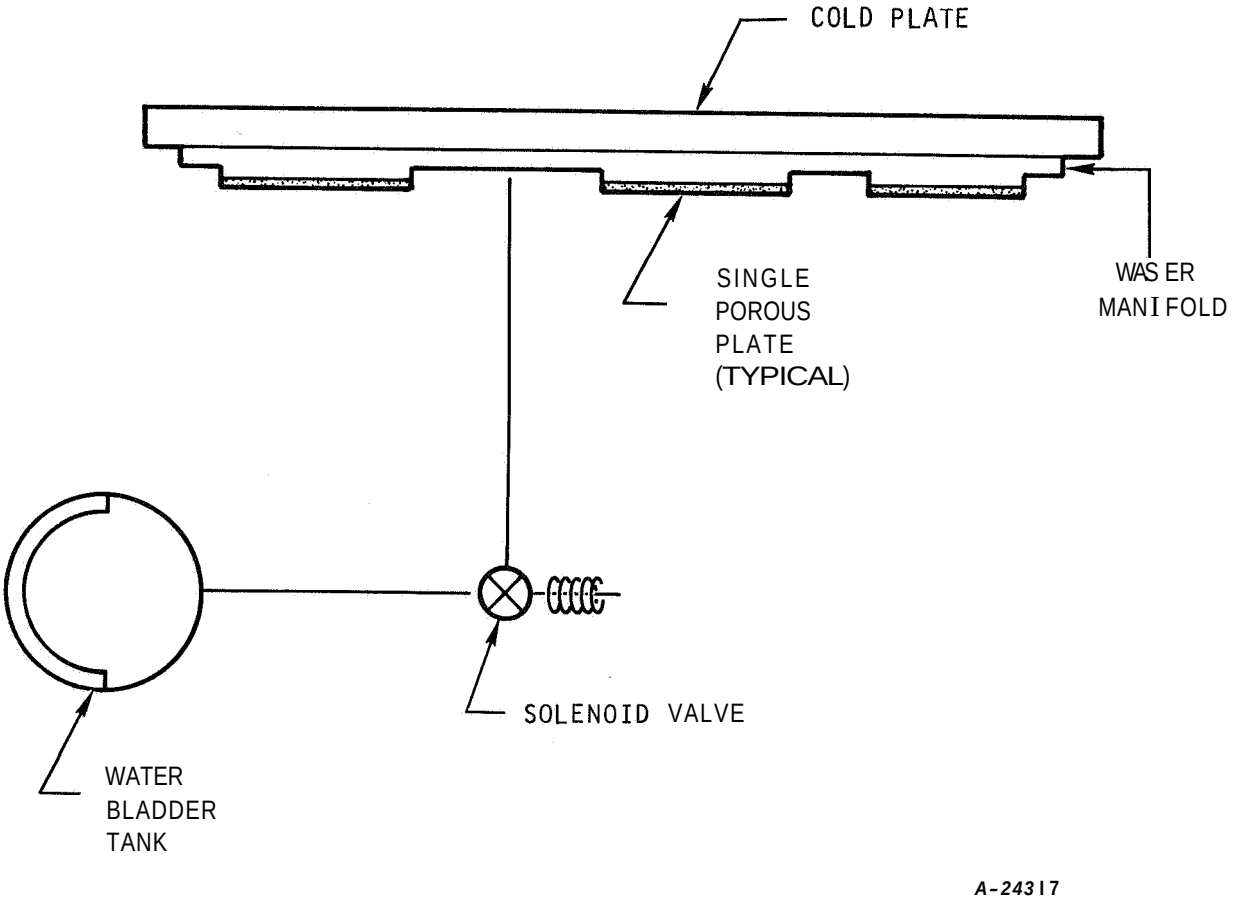

Figure 19. Simple Subl imator System

Simple Wick Boiler

Figure 20 shows a conceptual design of a simple wick boiler, consisting of a wick attached to the cold plate, and a steam back pressure valve. The wick is initially saturated with sufficient water to meet the required heat load. When the heat load is applied, the steam back pressure valve is opened, reducing the plenum pressure and allowing the water in the wick to boil. When the heat load is reduced or eliminated, the back pressure valve is closed, reducing or terminating boiling. The system may be easily restarted since there is no freezing involved. The wick may cover the entire cold plate or may be contoured to cover only the areas of greatest heat flux. The steam back pressure may be controlled by one of several methods; thermistors may be used to sense the plate temperature at various critical locations, a Freon filled bulb imbedded in the cold plate would function like a typical expansion valve to control the back pressure, or a steam temperature-sensing Vernatherm-actuated valve might be used.

Wax Heat Sink Unit

Figure 21 is a sketch of a design which is a somewhat different concept than a sublimator or boiler, a wax heat sink unit. This design, which consists of a wax or similar substance with a suitable melting point encapsulated in a finned or honeycomb passage, is quite attractive for small heat loads due to the simplicity of operation. When the heat load is applied to the cold plate, the wax acts as a heat sink by melting. No controls of any type are needed for this design; however, it is limited to small heat loads. It is possible to obtain only about 80 Btu of cooling per lb of wax, whereas with a water boiler or sublimator, about 1000 Btu per lb of water is available. The water/methanol precooling fluid passage shown in the sketch may be connected to the spacecraft cooling system to cool the equipment during launch and to assure that the wax is in a solid state prior to its use as a heat sink.

Heat Pipe System

Figure 22 is a sketch of a heat pipe thermal panel system. This design incorporates a wick and vapor manifold covering the cold plate and extending

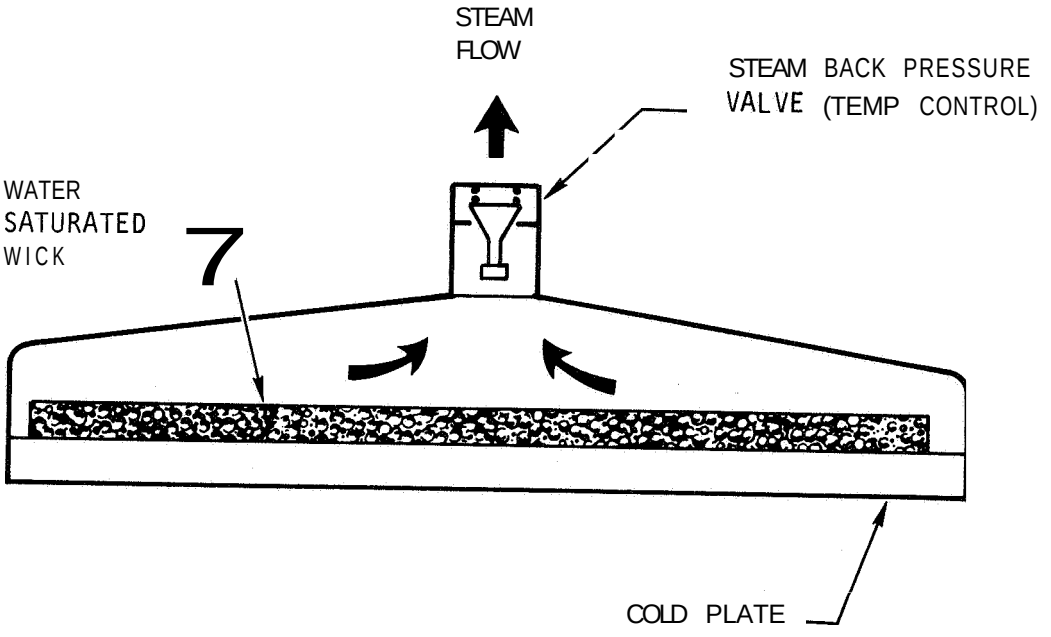

Figure 20. Simple **Wick** Boiler

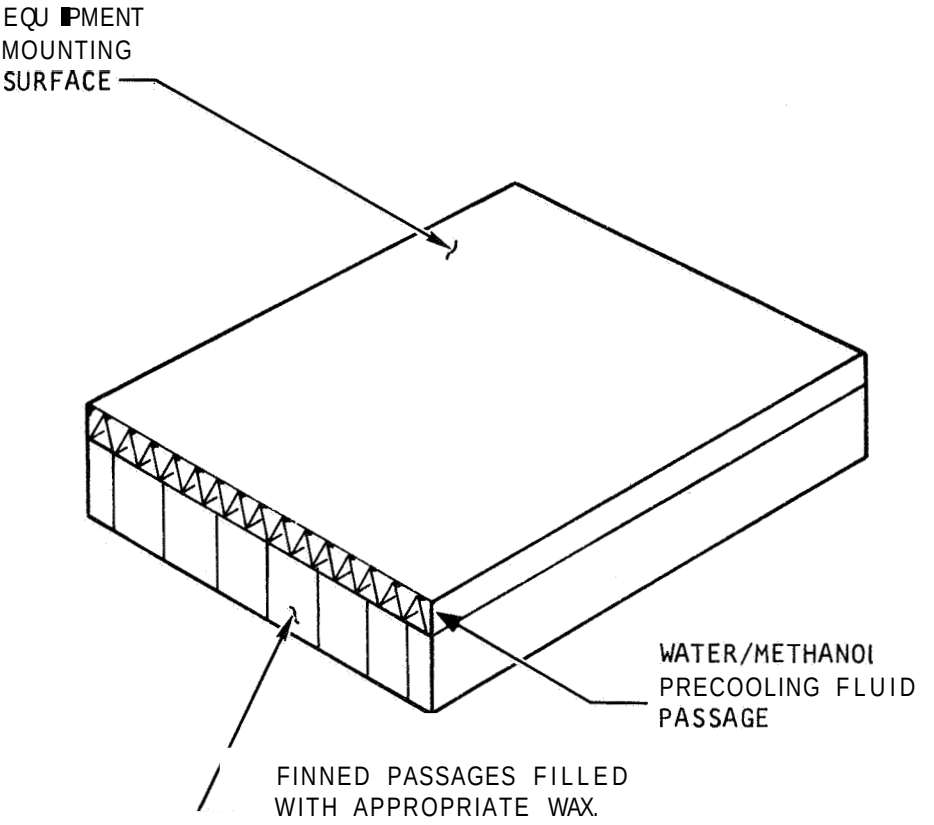

Figure 21. Wax Heat Sink Unit

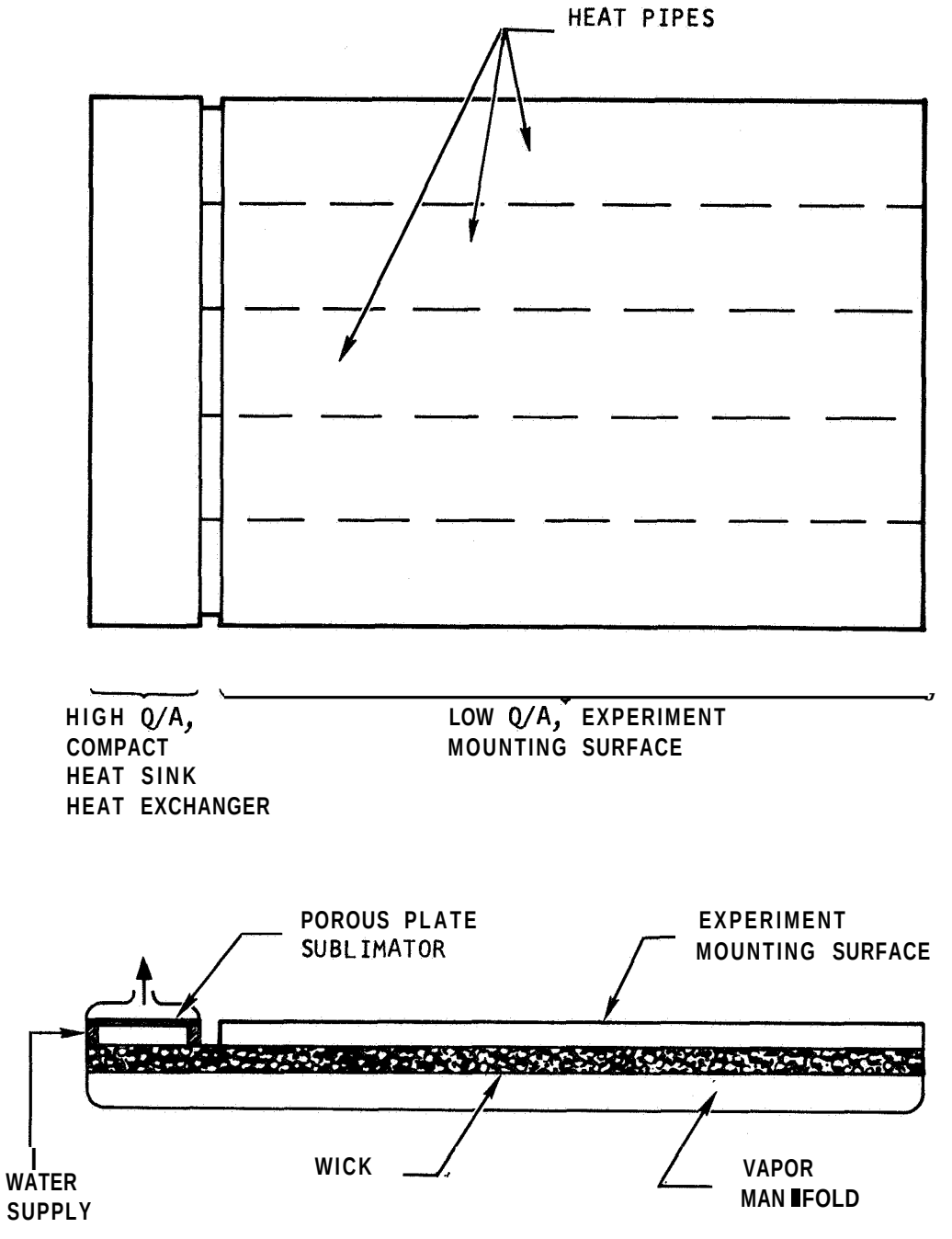

Figure 22. Heat Pipe System

past the plate to a compact heat sink heat exchanger, in this case, a porous plate sublimator. The wick is initially saturated with water. When a heat load is applied, the water boils at the heat load and more water is transported from the cold end of the panel, that area adjacent to the sublimator. The vapor generated in boiling is condensed at the cold end so that there is a continuous circulation of liquid water through the wick and vapor through the manifold. Water from a remote supply is sublimed in the sublimator in condensing the vapor in the heat pipe. Just as in the simple wick design, nonuniform heat fluxes may be handled sufficiently well in a heat pipe design because more water is transported to the high heat flux regions.

The controls for this system would be similar to those in a simple sublimator since no controls are needed in the wick chamber.

Regenerative Coolant **Loop** System With Gelatin Sublimator

Figure 23 is a schematic of a regenerative coolant loop system. In this design a pump circulates the coolant (water/methanol, for instance) through the cold plate and through a sublimator where the coolant loses heat, cooling the cold plate. In order to reduce the problem of congealing or freezing of the heat transport fluid, all the coolant is passed through the sublimator, and temperature control is achieved by bypassing some of the fluid past the regenerator. The heat sink in this design is a sublimator, either the conventional water-fed type or a "gelatin sublimator." The gelatin sublimator consists of a honeycomb passage filled with gelatin, a solid state sublimant, and a flow passage through with the water/methanol passes. The gelatin is directly exposed to space vacuum (no porous plate is used) and sublimes, just as ice does in a conventional water fed sublimator. Under these conditions very low equilibrium sublimation temperatures will be encountered; at low heat loads the sink temperature could be below -60°F. The gelatin type of subliming material may be incorporated in any of the sublimator designs and is not peculiar to this particular circulating flow scheme. Since no porous plates are used with the gelatin design, the sublimator is free of any potential plugging problems. All gelatin required for a particular mission must be initially stored in the sublimator. The face of the

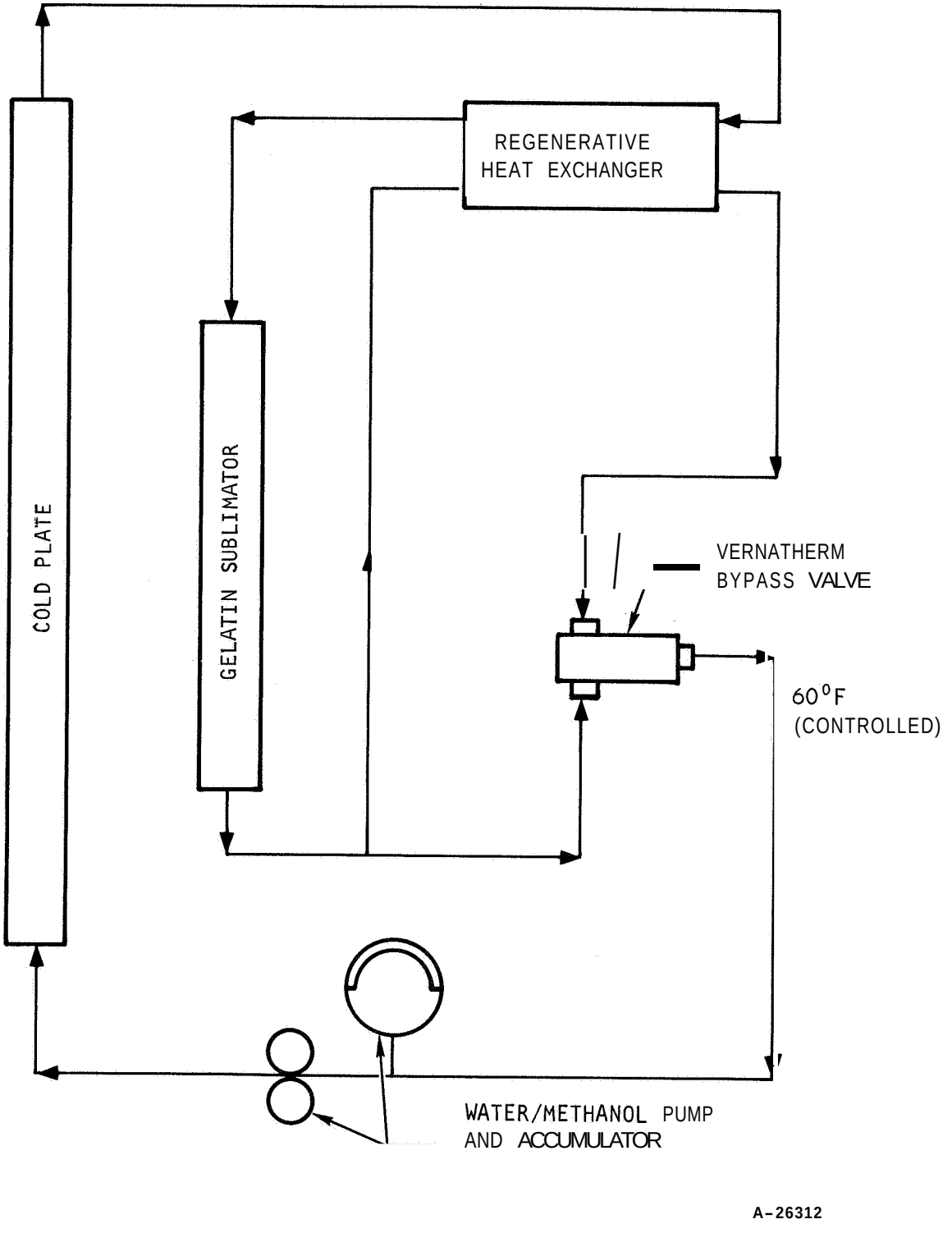

Figure 23. Regenerative Coolant Loop System

sublimator is completely exposed to space; hence, the gelatin consistency must be adequate to withstand the rigors of launch. After completing a mission, a fine powder will remain in the unit which must be removed prior to reuse. For ease of operation, the sublimator can be designed to use a replaceable gelatin cartridge.

Possible disadvantages of this system are the need for a pump to circulate the coolant and the added weight of a regenerative heat exchanger.

Remote Wick Boiler

Another type of thermal panel design which requires a pump loop is the remote wick boiler design, called such because the wicks need not be directly adjacent to the cold plate. Figure *24* illustrates a typical boiler and water reservoir design which incorporates an ordinary wick-type boiler core integrated with a wick lined water reservoir. The coolant loop to the cold plate is not shown in this case, however, it would include a pump and accumulator as in the regenerative coolant loop concept. This would allow the heat sink to be located remote to the cold plate if so desired. The wick-lined water reservoir feeds water to the boiler core with no water carryover. The water demand is self-controlling and boiling temperature is controlled with a back-pressure valve. A regenerative heat exchanger is not required in this design since there is no chance of freezing the coolant. Since no ice is formed in the system, no problems with zero heat load and restart are anticipated.

Combined Subliming and Transport Fluid System

The design shown in Figure 25 combines the heat transport fluid and the subliming fluid into the same flow loop. The water is heated as it passes through the cold plate and is cooled as it passes through the sublimator by subliming itself. Temperature control is achieved by bypassing some of the water around the sublimator and makeup water is supplied from a Freon pressurized water bladder tank. It is possible that this system would be difficult to restart after a long quiescent period due to water freezing in the sublimator and in its inlet and outlet lines.

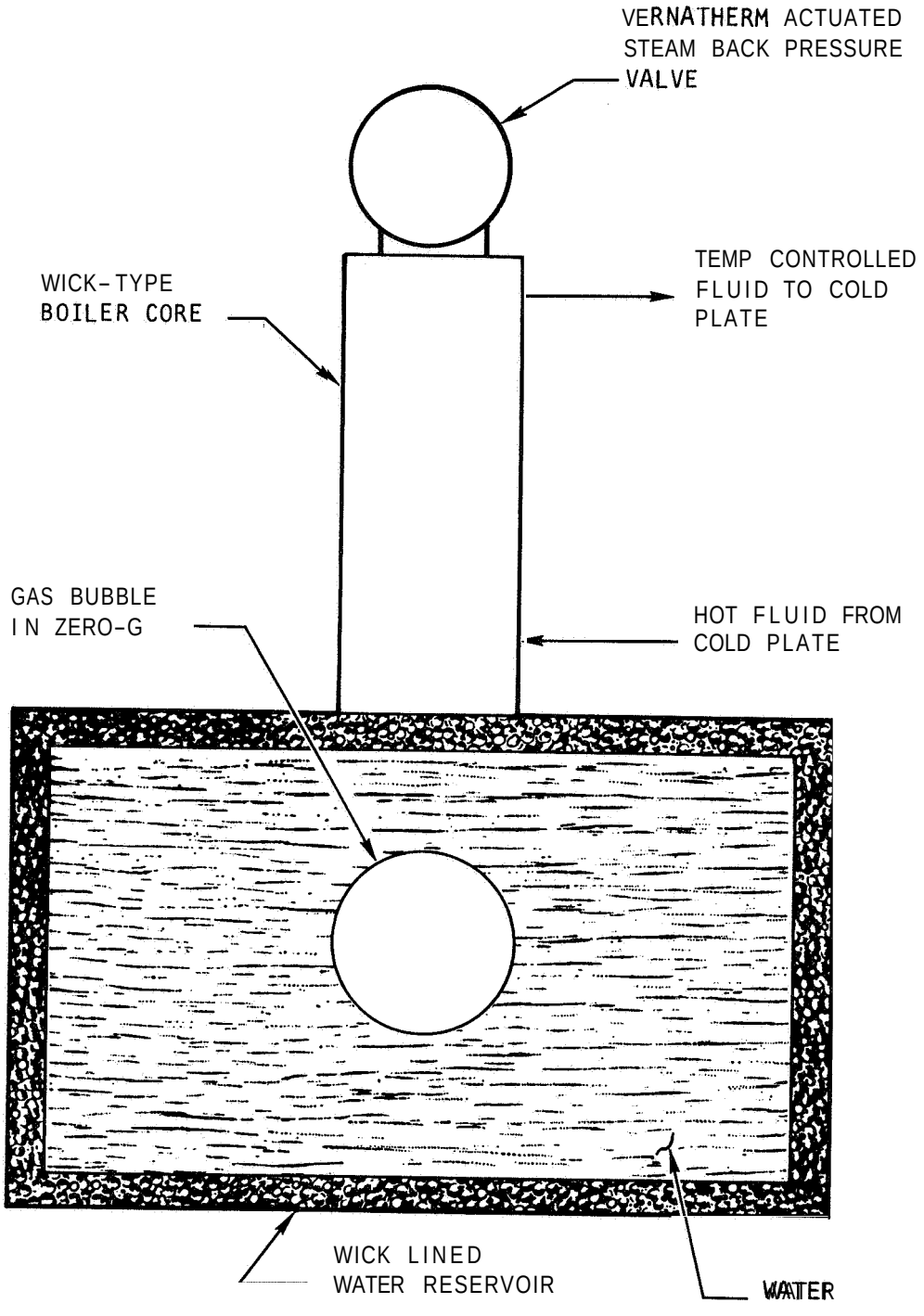

Figure 24. Remote Wick Boiler

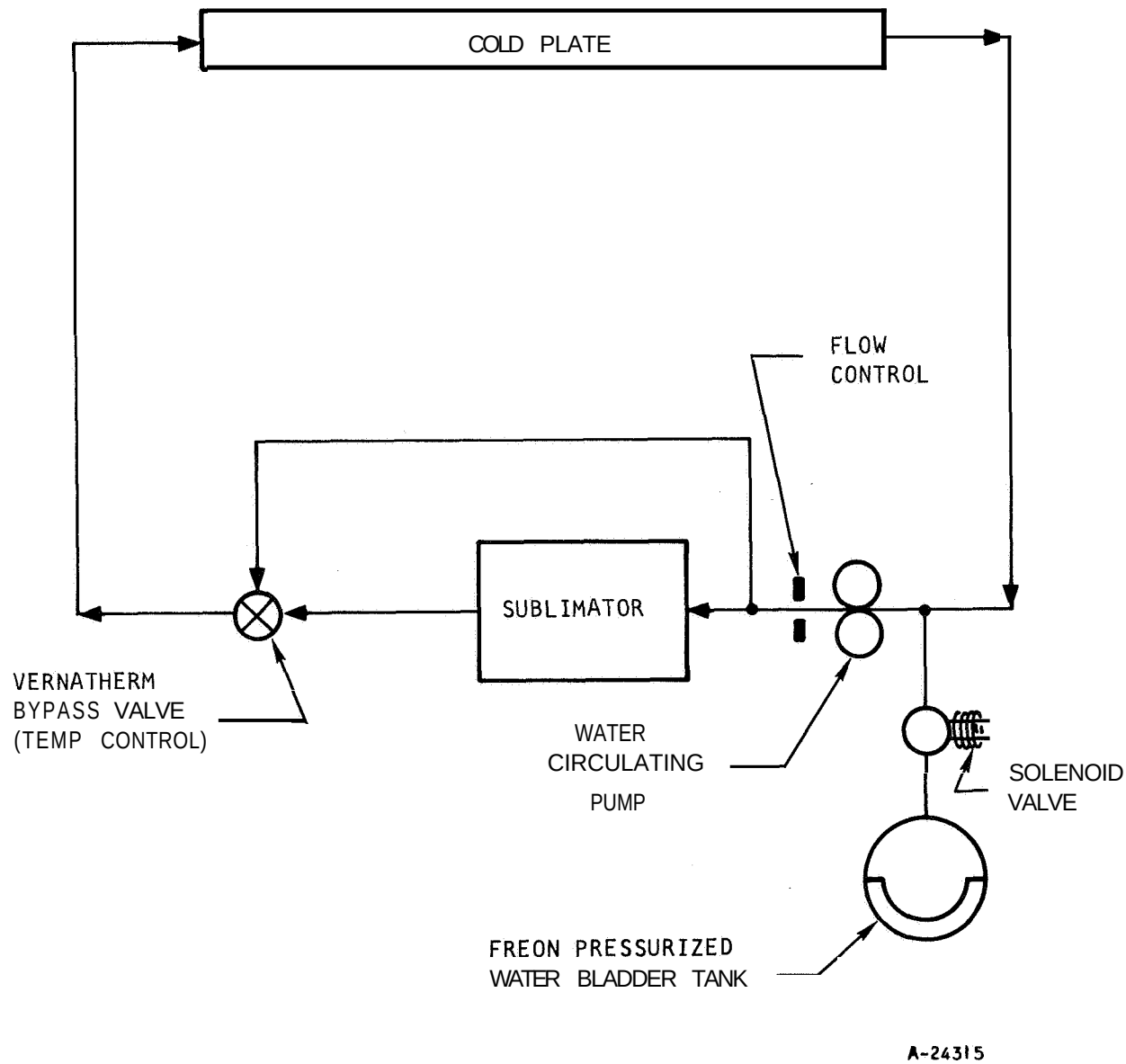

Figure **25.** Combined Subliming and Transport Fluid System

Wick Boiler System

Another thermal panel wick boiler configuration is shown in Figure 26. In this design, water is stored in a reservoir containing a pliable bladder or diaphragm. The diaphragm allows volume expansion when ice is formed and also functions to expel water under pressure as the heat load increases. The expulsion is accomplished by the vapor pressure of a suitably chosen fluid, such as Freon, when temperature increases to a point at which pressure unseats the spring-loaded poppet in the water feed line. The vapor pressure working on one side of the bladder and the spring load on the valve then establish the temperature control of the panel. The water discharge through the poppet is vaporized on the heat transfer surface. There is some question as to whether sufficient heat transfer can be provided to the Freon in the absence of natural convection due to operation in zero g.

FUTURE ACTIVITIES

During the next quarter it is planned to proceed with a revised development plan. Specific areas to be covered for each phase of the program are outlined below.

Water Boiler Heat Sink Module

a. Basic wick performance testing designed to establish optimum wick characteristics will be completed on the variable area boiler test rig.

b, Controls analysis including water feed control and distribution will be performed and a control system designed and built.

c. A one kilowatt boiler test unit will be designed and built.

d. Layout design studies on module stacking to meet a six kilowatt load will be conducted.

e. Parametric studies of boiler performance will be performed.

Sublimator Heat Sink Module

a. Start-up, shutdown, and restart tests of single module sublimators will be performed.

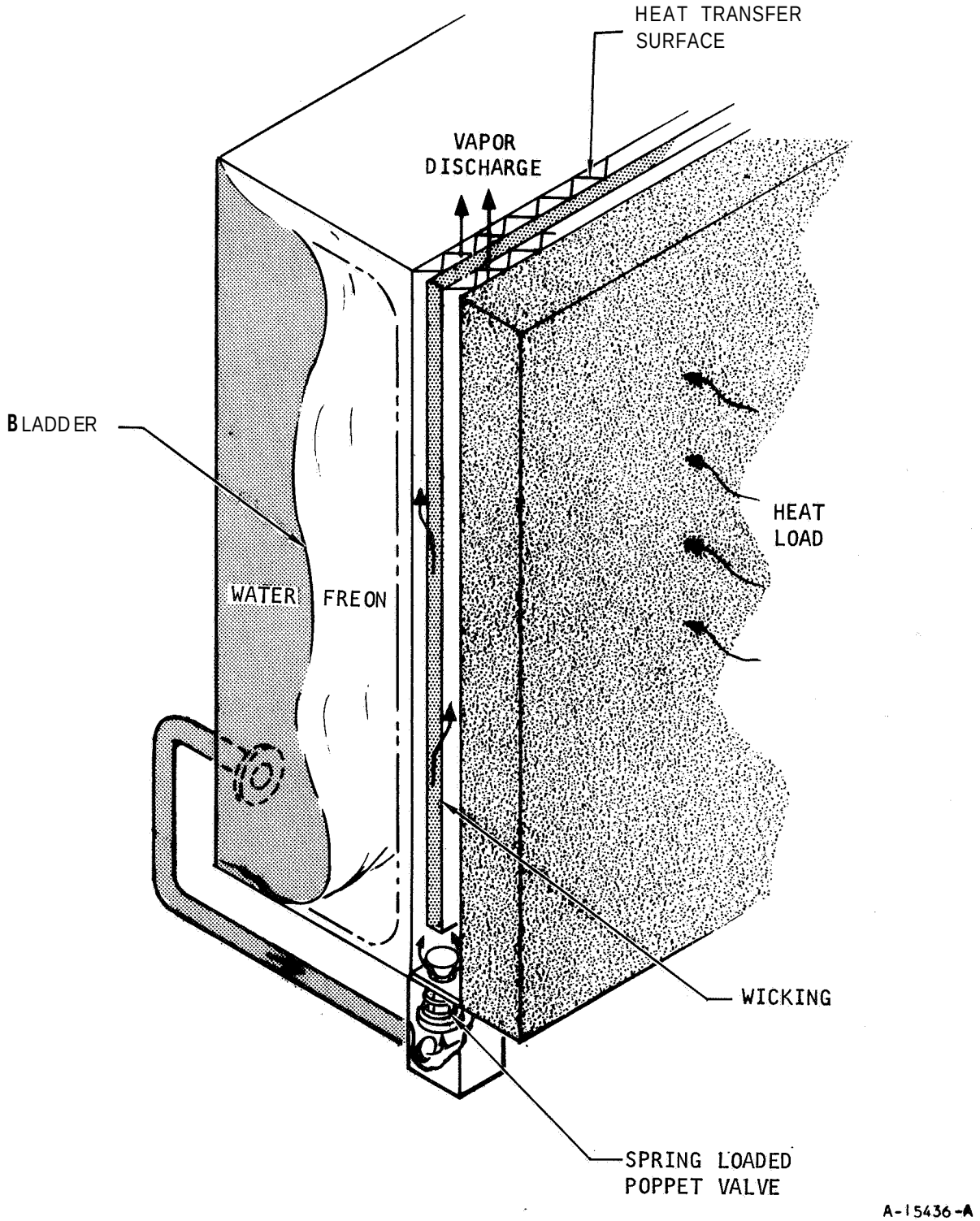

Figure 26. Wick Boiler System

b. Performance tests of hydrophobic porous plates will be initiated.

c. A one kilowatt sublimator test unit will be designed and built.

d. Parametric analysis of the freezing problem and effect of steam passage dimensions will be performed.

Thermal Panel Development

a. Preliminary thermal panel concepts will be analyzed and revised, and one or two designs selected for development.

b. The selected concepts will be analyzed parametrically and small test units will be designed, fabricated, and tested.